Table 6 (*continued*)

	Normal ALT n = 891		Elevated ALT n = 239		Univariate test	*P* value	Multivariate test			
							OR[a]	95% CI		*P* value
	n	%	n	%				Upper	Lower	
High (>18)	6	(.7)	6	(2.5)						
HOMA-IR										
0-1.9	731	(82.0)	130	(54.4)	M	<.001	1.00			
2.0-3.9	148	(16.6)	94	(39.3)			2.44	1.68	3.55	<.001
≥4	12	(1.3)	15	(6.3)			4.93	2.14	11.33	<.001
Blood pressure										
Normal	336	(37.7)	67	(28.0)	C	.006				
Hypertension	555	(62.3)	172	(72.0)						
Smoking habit										
Never	821	(92.1)	221	(92.5)	C	.494				
Current	44	(4.9)	14	(5.9)						
Former	26	(2.9)	4	(1.7)						
Drinking habit										
Never or former	760	(85.3)	210	(87.9)	C	.312				
Current	131	(14.7)	29	(12.1)						
Current medication[b]										
No	879	(98.7)	237	(99.2)	F	.746				
Yes	12	(1.3)	2	(0.8)						

[a] Multiple logistic regression analysis. Age group and the variables with *P* less than .1 on univariate analysis were included in the model.
[b] Current medication for hypertension, lipid metabolism abnormality, and diabetes was excluded.

of 957 men, and 188 (16.6%) of 1130 women. The ALT levels in these subjects were 29.2 ± 17.9 U/L in men and 24.1 ± 13.4 U/L in women; and thus, the mean levels were close to the cutoff values determined in this study. These values were significantly higher than those for subjects who had 0 or 1 metabolic risk factor for both men and women ($P < .001$) (Table 4).

3.6. Factors associated with elevated ALT levels

Factors associated with elevated ALT higher than the upper limits were investigated in 2087 subjects who were negative for anti-HCV antibody and serum hepatitis B surface antigen. The results for 957 men and 1130 women are shown in Tables 5 and 6, respectively. In men, 10 factors with a significant association with elevated ALT were identified in univariate analysis: age group, high γ-GTP, low adiponectin, high total cholesterol, high LDL cholesterol, high triglycerides, high BMI, high fasting glucose, high fasting insulin, and high HOMA-IR. In women, 10 factors associated with elevated ALT were identified in univariate analysis: high γ-GTP, low adiponectin, high total cholesterol, high LDL cholesterol, high triglycerides, high BMI, high fasting glucose, high fasting insulin, high HOMA-IR, and hypertension. A current drinking habit was not associated with elevated ALT in either men or women in univariate analysis. Multivariate logistic regression models were constructed for men and women using variables with low *P* values in univariate analysis. This analysis revealed 5 factors in men (high γ-GTP: odds ratio [OR], 5.57; 95% CI, 3.80-8.16; $P < .001$; low adiponectin: OR, 0.93; 95% CI, 0.88-0.98; $P < .02$; high LDL cholesterol: OR, 1.58; 95% CI, 1.06-2.35; $P < .03$; high BMI: OR, 1.85; 95% CI, 1.28-2.68; $P < .01$; and high HOMA-IR [2.0-3.9]: OR, 1.94; 95% CI, 1.26-2.98; $P < .01$; [≥4]: OR, 2.94; 95% CI, 1.26-6.86; $P < .02$) and 4 factors in women (high γ-GTP: OR, 11.54; 95% CI, 6.12-21.75; $P < .001$; low adiponectin: OR, 0.97; 95% CI, 0.93-1.00; $P < .05$; high BMI: OR, 2.02; 95% CI, 1.43-2.84; $P < .001$; and high HOMA-IR [2-3.9]: OR, 2.44; 95% CI, 1.68-3.55; $P < .001$; [≥4]: OR, 4.93; 95% CI, 2.14-11.33; $P < .001$) with a significant association with elevated ALT levels.

4. Discussion

Elevated serum ALT levels in the general population are closely associated with NAFLD, which is a liver phenotype of metabolic syndrome [4-8]. Alanine aminotransferase activities have also been shown to be useful as an indicator of general health [14], and ALT is a predictor of mortality in community residents [13]. Mortality may be due to unrecognized liver diseases, but may also be due to other causes of ALT elevation, such as atherosclerosis, hypertension, and type 2 diabetes mellitus, which are linked to nonliver health risks. This suggests the importance of determining the association of ALT levels with metabolic factors influencing the occurrence of metabolic syndrome–related diseases in a large population sample. Our results clearly indicate that elevated ALT levels unrelated to hepatitis virus infection are closely associated with metabolic syndrome–related features in a study population that is representative of the general Japanese population older than 40 years old. This suggests that measurement of ALT levels is likely to be a useful primary screening test for metabolic syndrome in the population.

In this study, the seroprevalences of hepatitis B and C were 1.7% and 1.9%, respectively, similar to the standard rates in the Japanese population [22]. Because hepatitis B and C infection is associated with elevated ALT levels, subjects positive for hepatitis markers were excluded from further analysis. To date, the upper limits of ALT levels in screening tests for the general population have not been established clearly; and therefore, we reevaluated these limits for effective screening of metabolic syndrome in the Japanese adult population. Previous reports have shown that sex has a significant influence on ALT levels [23,24]; and therefore, we assessed ALT levels separately for men and women. The ALT cutoff levels for effective screening of individuals with metabolic syndrome for men and for women were proposed in this study on the basis of the relationship between ALT levels and the number of the 3 major metabolic risk factors. Upper limits of 30 U/L in men and 25 U/L in women gave a good specificity of more than 80% for exclusion of subjects with none or 1 of the 3 metabolic risk factors: hypertension, lipid metabolism abnormality, and hyperglycemia. Using these cutoff values, we demonstrated that approximately 20% of the male and female subjects older than 40 years had ALT elevation. A current drinking habit was identified in 694 (72.5%) of 957 men and 160 (14.3%) of 1130 women, but a drinking habit itself was not significantly associated with elevated ALT in univariate analyses in this population, although there is no doubt that excess intake of alcohol causes liver injury in each individual. Multivariate analysis clearly showed that metabolic syndrome–related features that reflect obesity and insulin resistance, including high BMI, high LDL cholesterol, high HOMA-IR, and lower adiponectinemia, were associated with elevated ALT in the study population.

Elevated serum γ-GTP also showed a significant association with elevated ALT in both male and female subjects. These results were replicable in subjects without a history of alcohol consumption (data not shown). Previous studies have documented that elevated serum γ-GTP has a risk for metabolic syndrome and type 2 diabetes mellitus in middle-aged Japanese male office workers [25] and may represent an early marker of subclinical inflammation and increased oxidative stress in healthy individuals [26,27]. Our results are consistent with these studies, and we also found that elevated γ-GTP was associated with obesity and insulin resistance in both men and women. Therefore, γ-GTP is a promising marker for metabolic syndrome and particularly for prediction of development of metabolic syndrome–related diseases; and this warrants a further prospective study.

Because high serum ALT levels often reflect hepatic fat accumulation and inflammation, they are well correlated with the prevalence of NAFLD in the population in cases of unexplained ALT elevation. The importance of ALT activity as an indicator of NAFLD has been demonstrated in association with metabolic abnormalities caused by central obesity and insulin resistance [28-30]. Nonalcoholic fatty liver disease is classified into 2 categories: simple fatty liver and nonalcoholic steatohepatitis (NASH), which is intractable and progressive. The population with elevated ALT levels includes those with NASH [7,8,31] as a phenotype of metabolic syndrome in the liver. Fat droplets in liver tissue are often depleted in the advanced stage of NASH, and such cases may be diagnosed as cryptogenic liver cirrhosis or liver cancer [32]. In fact, the prevalence of obesity, hypertriglyceridemia, or type 2 diabetes mellitus is significantly higher in cases of liver cancer that develop from cryptogenic cirrhosis compared with those caused by HCV infection or excess intake of alcohol [33]. Because a cohort study showed prospectively that individuals with NAFLD had a higher mortality due to liver disease–related deaths [34], people in the general population with high ALT levels are of particular concern because those with NASH have a risk for progression to cirrhosis or cancer.

Individuals with minor elevation of serum ALT levels that are close to the upper limits of the reference range are also of concern because elevated ALT itself is closely associated with insulin resistance, even in the absence of NAFLD and obesity [35,36]. Recent studies have shown that elevated ALT could be a prognostic marker for development of metabolic syndrome [11,12]. Because individuals with ALT elevation have a potential risk for development of various metabolic syndrome–related diseases, including type 2 diabetes mellitus [9], cardiovascular disease [10], atherothrombosis [37], and obstructive sleep apnea [38], it may be worthwhile to notify those with minor ALT elevation of the risk of such diseases. In fact, in this study, we found that mean ALT activities in subjects with 2 or 3 metabolic risk factors were not particularly high, tending only to be close to the upper limit. Thus, minor ALT elevation is also an important feature for effective screening of metabolic syndrome. Elevation of ALT beyond the cutoff levels determined in this study was strongly associated with a broad spectrum of metabolic syndrome–related features, including obesity and insulin resistance. A prospective study of the association between elevated ALT levels and the occurrence of metabolic syndrome–related diseases is now in progress in this Takahata cohort, which includes more than 4000 people and is representative of the Japanese adult population.

In conclusion, the results of this study clearly show that elevated ALT levels in the Japanese population older than 40 years are associated with obesity and insulin resistance, which in turn are associated with metabolic syndrome. This suggests that, in addition to detection of liver disease, screening of serum ALT levels may contribute to identifying the potential risk of metabolic syndrome–related diseases in the general population.

Acknowledgment

This study was supported by a Grant-in-Aid from the Center of Excellence program of the Japan Society for the Promotion of Science.

References

[1] Matsuzawa Y. The metabolic syndrome and adipocytokines. FEBS Lett 2006;580:2917-21.

[2] Kawata S. Association of digestive organ disease with metabolic syndrome: role of adipocytokine and its molecular mechanisms. Clin J Gastroenterol 2008;1:1-6.

[3] Russo A, Autelitano M, Bisati L. Metabolic syndrome and cancer risk. Eur J Cancer 2008;44:293-7.

[4] Bedogni G, Miglioli L, Masutti F, et al. Prevalence of and risk factors for nonalcoholic fatty liver disease: the Dionysos nutrition and liver study. Hepatology 2005;42:44-52.

[5] Bellentani S, Tiribelli C, Saccoccio G, et al. Prevalence of chronic liver disease in the general population of northern Italy: the Dionysos study. Hepatology 1994;20:1442-9.

[6] Liu CM, Tung TH, Liu JH, et al. A community-based epidemiological study of elevated serum alanine aminotransferase levels in Kinmen, Taiwan. World J Gastroenterol 2005;11:1616-22.

[7] Liangpunsakui S, Chalasani N. Unexplained elevations in alanine aminotransferase in individuals with the metabolic syndrome: results from the third National Health and Nutrition Survey (NHANES III). Am J Med Sci 2005;329:111-6.

[8] Ioannou GN, Boyko EJ, Lee SP. The prevalence and predictors of elevated serum aminotransferase activity in the United States in 1999-2002. Am J Gastroenterol 2006;101:76-82.

[9] Vozarova B, Stefan N, Lindsay RS, et al. High alanine aminotransferase is associated with decreased hepatic insulin sensitivity and predicts the development of type 2 diabetes. Diabetes 2002;51:1889-95.

[10] Schindhelm RK, Dekker JM, Nijpels G, et al. Alanine aminotransferase predicts coronary heart disease events: a 10-year follow-up of the Hoorn Study. Atherosclerosis 2007;191:391-6.

[11] Hanley AJG, Williams K, Festa A, et al. Liver markers and development of the metabolic syndrome. The insulin resistance atherosclerosis study. Diabetes 2005;54:3140-7.

[12] Schindhelm RK, Dekker JM, Nijpels G, et al. Alanine aminotransferase and the 6-year risk of the metabolic syndrome in Caucasian men and women: the Hoorn Study. Diabet Med 2007;24:430-5.

[13] Hoon Lee T, Ray Kim W, Benson JT, et al. Serum aminotransferase activity and mortality risk in a United States community. Hepatology 2008;47:880-7.

[14] Ray Kim W, Flamm SL, Di Bisceglie AM, et al. Serum activity of alanine aminotransferase (ALT) as an indicator of health and disease. Hepatology 2008;47:1363-70.

[15] Park YW, Allison DB, Heymsfield SB, et al. Larger amounts of visceral adipose tissue in Asian Americans. Obes Res 2001;9:381-7.

[16] Bonora E, Targher G, Alberiche M, et al. Homeostasis model assessment closely mirrors the glucose clamp technique in the assessment of insulin sensitivity: studies in subjects with various degrees of glucose tolerance and insulin sensitivity. Diabetes Care 2000;23:57-63.

[17] Romero-Gomez M, Del Mar Viloria M, Andrade RJ, et al. Insulin resistance impairs sustained rate to peginterferon plus ribavirin in chronic hepatitis C patients. Gastroenterology 2005;128:636-41.

[18] Grundy SM, Cleeman JI, Daniels SR, et al. Diagnosis and management of the metabolic syndrome. An American Heart Association/National Heart, Lung, and Blood Institute scientific statement. Circulation 2005;112:2735-52.

[19] Arai H, Yamamoto A, Matsuzawa Y, et al. Prevalence of metabolic syndrome in the general Japanese population in 2000. J Atheroscler Thromb 2006;13:202-8.

[20] van der Poorten D, Kenny DT, Butler T, et al. Liver disease in adolescents: a cohort study of high-risk individuals. Hepatology 2007; 46:1750-8.

[21] Prati D, Taioli E, Zanella A, et al. Updated definitions of healthy ranges for serum alanine aminotransferase levels. Ann Intern Med 2002;137: 1-10.

[22] Tanaka J, Kumagai J, Katayama K, et al. Sex- and age-specific carriers of hepatitis B and C viruses in Japan estimated by the prevalence in the 3,485,648 first-time blood donors during 1995-2000. Intervirology 2004;47:32-40.

[23] Elinav E, Ben-Dov IZ, Ackerman E, et al. Correlation between serum alanine aminotransferase activity and age: an inverted U curve pattern. Am J Gastroenterol 2005;100:2201-4.

[24] Kariv R, Leshno M, Beth-Or A, et al. Re-evaluation of serum alanine aminotransferase upper normal limit and its modulating factors in a large-scale population study. Liver Int 2006;26:445-50.

[25] Nakanishi N, Suzuki K, Tatara K. Serum gamma-glutamyltransferase and risk of metabolic syndrome and type 2 diabetes in middle-aged Japanese men. Diabetes Care 2004;27:1427-37.

[26] Bo S, Gambino R, Durazzo M, et al. Association between gamma-glutamyl transferase, metabolic abnormalities and inflammation in healthy subjects from a population-based cohort: a possible implication for oxidative stress. World J Gastroenterol 2005;11:7109-17.

[27] Yamada J, Tomiyama H, Yambe M, et al. Elevated serum levels of alanine aminotransferase and gamma glutamyltransferase are markers of inflammation and oxidative stress independent of the metabolic syndrome. Atherosclerosis 2006;189:198-205.

[28] Oh SY, Cho YK, Kang MS, et al. The association between increased alanine aminotransferase activity and metabolic factors in nonalcoholic liver diseases. Metabolism 2006;55:1604-9.

[29] Suzuki A, Angulo P, Lymp J, et al. Chronological development of elevated aminotransferase in a nonalcoholic population. Hepatology 2005;41:64-71.

[30] Fan JG, Li F, Cai XB, et al. Effects of nonalcoholic fatty liver disease on the development of metabolic disorders. J Gastroenterol Hepatol 2007;22:1086-91.

[31] Ioannou GN, Weiss NS, Boyko EJ, et al. Contribution of metabolic factors to alanine aminotransferase activity in persons with other causes of liver diseases. Gastroenterology, 2005;128:627-35.

[32] Marrero JA, Fontana RJ, Su GL, et al. NAFLD may be a common underlying liver disease in patients with hepatocellular carcinoma in the United States. Hepatology 2002;36:1349-54.

[33] Bugianesi E, Leone N, Vanni E, et al. Expanding the natural history of nonalcoholic steatohepatitis: from cryptogenic cirrhosis to hepatocellular carcinoma. Gastroenterology 2002;123:134-40.

[34] Adams LA, Lymp JF, St Sauver J, et al. The natural history of nonalcoholic fatty liver disease: a population-based cohort study. Gastroenterology 2005;129:113-21.

[35] Hanley AJ, Wagenknecht LE, Festa A, et al. Alanine aminotransferase and directly measured insulin sensitivity in a multiethnic cohort: the insulin resistance atherosclerosis study. Diabetes Care 2007;30: 1819-27.

[36] Saiazar MR, Carbajal HA, Curciarello JO, et al. Alanine-aminotransferase: an early marker for insulin resistance? Medicine (B Aires) 2007;67:125-30.

[37] Kain K, Carter AM, Grant PJ, et al. Alanine aminotransferase is associated with atherothrombotic risk factors in a British South Asian population. J Thromb Haemost 2008;6:737-41.

[38] Norman D, Bardwell WA, Arosemena F, et al. Serum aminotransferase levels are associated with markers of hypoxia in patients with obstructive sleep apnea. Sleep 2008;31:121-6.

Therapeutic Apheresis and Dialysis

Therapeutic Apheresis and Dialysis 13(6):509–514
doi: 10.1111/j.1744-9987.2009.00779.x

Biological Effect of Anaphylatoxin C5a on the Generation of Anti-inflammatory Substances in Leukocyte Adsorption

Shoichi Nishise,[1] Yuji Takeda,[2] Yuko Nishise,[1] Shoichiro Fujishima,[1] Tomohiko Orii,[1] Sayaka Otake,[1] Takeshi Sato,[1] Yu Sasaki,[1] Hiroaki Takeda,[1] and Sumio Kawata[1]

[1]*Department of Gastroenterology, Yamagata University School of Medicine, Yamagata, and* [2]*Department of Environmental and Preventive Medicine, Hyogo College of Medicine, Nishinomiya, Japan*

Abstract: Anaphylatoxins, which are involved in both pro-inflammatory processes and a variety of anti-inflammatory effects, are produced during granulocyte and monocyte adsorptive apheresis. We noticed the anti-inflammatory effects of C5a, the strongest anaphylatoxin, in granulocyte and monocyte adsorptive apheresis. The aim of this study was to investigate the effect of C5a on interleukin-1 receptor antagonist (IL-1ra) and hepatocyte growth factor (HGF) generation in granulocyte and monocyte adsorption. Peripheral blood containing nafamostat mesilate as an endogenous complement activation inhibitor was divided into four groups: (1) no recombinant C5a added, no contact with cellulose acetate (CA) beads (control group); (2) no C5a added, contact with CA beads; (3) C5a added, no contact with CA beads; and (4) C5a added, contact with CA beads. After incubation, IL-1ra and HGF in plasma were measured. IL-1ra was significantly higher in group 3, in which only C5a was added in the absence of CA beads, compared to groups 2 ($P < 0.01$) and 4 ($P < 0.05$). HGF was significantly higher only in group 4, in which C5a was added in the presence of CA beads ($P < 0.05$), but did not increase in the absence of CA beads. C5a can directly induce IL-1ra generation without the granulocyte and monocyte adsorption stimuli to CA beads, but can synergistically induce HGF generation with the adsorption stimuli, indicating C5a has different effects on IL-1ra and HGF generation.
Key Words: Adsorption, Apheresis, Complement C5a, Granulocyte, Hepatocyte growth factor, Interleukin-1 receptor antagonist.

A granulocyte and monocyte (GM) adsorptive apheresis (GMA) device (Adacolumn; JIMRO Institute, Takasaki, Japan) can deplete excess and activated GMs from the peripheral blood of patients with ulcerative colitis (UC) (1,2) and rheumatoid arthritis (3). The device comprises a column filled with 2 mm cellulose acetate (CA) beads that act as carriers for adsorptive leukocyte apheresis (4). Steroid and GMA therapies are similarly effective in relieving the symptoms of UC patients, but the latter causes less severe side-effects (5,6). Therefore, characterization of the biological responses to GMA is useful to elucidate the physiological anti-inflammatory responses in patients with inflammatory diseases.

A decrease in GMs was initially considered to be important to the anti-inflammatory effect, but the cell numbers recover within approximately 24 h after GMA. Although the precise mechanisms of the clinical efficacy of GMA are unclear, GM adsorption possibly triggers various biological responses, such as the release of interleukin-1 receptor antagonist (IL-1ra) and hepatocyte growth factor (HGF) (4,7). These substances are returned to the patients along with the blood and might contribute to the restoration of normal immune function (8–10). We are interested in what type of stimulation is able to generate these anti-inflammatory substances in GMA.

Cellulose acetate was originally used in membrane-based hemodialysis devices (11–13) and it is known that CA membranes activate the complement system by contact with blood (11). Similarly, complement activation and generation of complement activation fragments containing anaphylatoxins

Received February 2009.
Address correspondence and reprint requests to Dr Shoichi Nishise, Department of Gastroenterology, Yamagata University School of Medicine, 2-2-2 Iida-nishi, Yamagata 990-9585, Japan. Email: nishise-sic@umin.ac.jp
Presented in part at the 29th Annual Meeting of the Japanese Society for Apheresis held November 21–23, 2008, in Hiroshima, Japan.

(such as C3a and C5a) are observed in the GMA column using CA beads (7,14,15). Anaphylatoxins C3a and C5a are known causes of pro-inflammatory processes (16–20); however, they are also involved in a variety of anti-inflammatory effects, including augmentation of anti-inflammatory cytokines (15,21,22).

GMA is a safe therapy for patients, without anaphylatoxin-induced side-effects. Thus, understanding the anti-inflammatory effects of anaphylatoxins in GMA is important for understanding the mechanisms of apheresis therapy. Based on this background, in this study we revealed the effects of complement C5a on the generation of anti-inflammatory substances (IL-1ra and HGF) in GMA.

MATERIALS AND METHODS

Reagents

Cellulose acetate beads were prepared by JIMRO Institute (Takasaki, Japan) and nafamostat mesilate was prepared by Torii Pharmaceutical (Tokyo, Japan). Recombinant human complement C5a (rhC5a) was purchased from Sigma (St Louis, MO, USA). All other chemicals were obtained commercially and were of the highest purity available.

Blood samples

After receiving written informed consent from all participants in the study, we collected peripheral blood from four healthy volunteers into plastic syringes (Terumo, Tokyo, Japan).

Exposure of blood to CA beads

A mixture of peripheral blood containing serial dilutions (1–100 μmol/L) of nafamostat mesilate, as anticoagulant and complement activation inhibitor, and CA beads at a 1:2 mL/g ratio in 10 mL syringes was rotated at 1 rpm for 1 h at 37°C. Blood samples were removed from the syringes by flash centrifugation at 80 × *g* for a few seconds. Fractions of granulocytes adsorbed to the CA beads were measured using a COULTER Gen-S hematology analyzer (Beckman Coulter, Fullerton, CA, USA), and then plasma separated by centrifugation at 800 × *g* for 5 min at 4°C was stored at −80°C. The ratio (%) of adsorbed granulocytes was calculated as follows: adsorbed granulocytes (%) = 100 × (number of granulocytes incubated without beads − number of granulocytes incubated with beads)/number of granulocytes incubated without beads. Cytotoxicity was examined by trypan blue exclusion assay.

Addition of rhC5a to complement activation inhibited blood

Peripheral blood containing 100 μmol/L nafamostat mesilate, which can almost completely inhibit both endogenous complement activation raised by contact between blood and CA beads and GM adsorption to CA beads (15), was divided into four groups: (1) no rhC5a added, no contact with CA beads (control group); (2) no rhC5a added, contact with CA beads; (3) 100 ng/mL rhC5a added, no contact with CA beads; and (4) 100 ng/mL rhC5a added, contact with CA beads. These were rotated at 1 rpm for 1 h at 37°C. The plasma was then separated and stored as mentioned above.

Measurement of anaphylatoxin C5a

Complement C5a was measured using a cytometric bead array anaphylatoxin kit (BD Biosciences, San Jose, CA, USA) with a flow cytometer (FACSCalibur; BD Biosciences) according to the manufacturer's instructions. The ratio (%) of increased C5a was calculated as follows: increased C5a (%) = 100 × (concentration of C5a after incubation − concentration of C5a before incubation)/concentration of C5a before incubation.

Measurement of IL-1ra and HGF

IL-1ra and HGF were measured using enzyme-linked immunosorbent assays (ELISAs) (R&D Systems, Minneapolis, MN, USA) according to the manufacturer's instructions. The optical density of test samples at 450 nm was determined using a Benchmark Plus microplate reader (Bio-Rad, Hercules, CA, USA). The ratio (%) of increased IL-1ra or HGF was calculated as follows: increased IL-1ra or HGF (%) = 100 × (concentration of IL-1ra or HGF after incubation − concentration of IL-1ra or HGF before incubation)/concentration of IL-1ra or HGF before incubation.

Statistical analysis

Statistical analyses proceeded as described in the figure legends, and $P < 0.05$ was considered significant. Data are presented as mean ± standard error (SE), unless otherwise noted.

RESULTS

Positive correlation between C5a increase and IL-1ra and HGF generation

We first verified the association between complement C5a increase and anti-inflammatory substance generation in the syringe filled with CA beads. Peripheral blood containing various concentrations (1–100 μmol/L) of nafamostat mesilate, serving not only as an anticoagulant but also as a complement activation inhibitor, was incubated with CA beads for 1 h to make various concentrations of complement

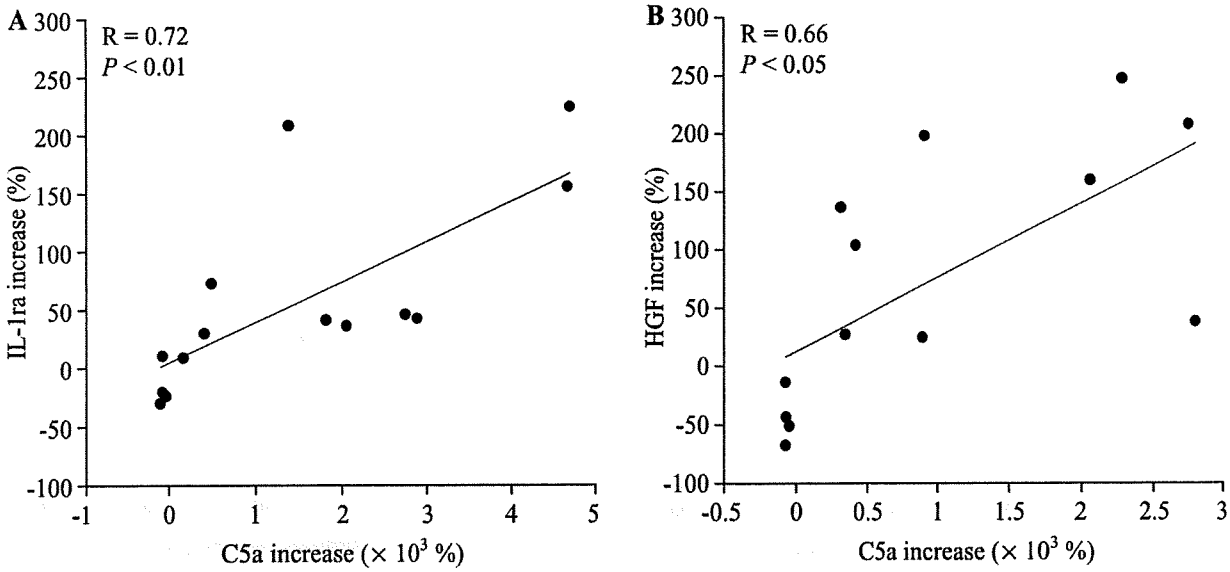

FIG. 1. Correlation of the increases in (A) interleukin-1 receptor antagonist (IL-1ra), and (B) hepatocyte growth factor (HGF) with C5a increase. Peripheral blood from healthy volunteers was mixed with serial dilutions of nafamostat mesilate. Test samples were then incubated with cellulose acetate beads for 1 h and the plasma was separated by centrifugation for the measurement of C5a, IL-1ra, and HGF after incubation. The increase ratios (%) of C5a, IL-1ra, and HGF were calculated as described in the Materials and Methods section. The *P* values are based on Spearman's rank correlation.

activation fragment C5a in blood. In the experiments described here, the number of granulocytes in the peripheral blood was 3236 ± 676.3 cells/μL. The C5a increase ratio was positively correlated with both the IL-1ra (Fig. 1A) and HGF (Fig. 1B) increase ratios. These results suggest that C5a generation is related to the generation of IL-1ra and HGF.

Effect of C5a on the generation of IL-1ra and HGF in GM adsorption

The C5a concentration in plasma reflects the degree of complement activation raised by contact between blood and CA beads, and complement activation induces GM adsorption to CA beads according to the degree of activation (15). Furthermore, the release of IL-1ra and HGF is related to the GMs absorbed to CA beads (7). In other words, the three phenomena (C5a generation, GM adsorption, and release of IL-1ra and HGF) are closely related. In this study, Figure 2A and B show that both IL-1ra and HGF increase ratios were positively correlated with the ratio of adsorbed granulocytes.

Previous reports were not enough to explain the relationship between C5a and the generation of IL-1ra and HGF, because C5a generation occurred simultaneously when GM adsorbed to CA beads in previous studies. Thus, to clarify the effect of C5a on the generation of IL-1ra and HGF, we prepared the complement inactive condition of blood using 100 μmol/L nafamostat mesilate and added rhC5a in the presence or absence of CA beads. We prepared four groups: (1) no rhC5a added, no contact with CA beads; (2) no rhC5a added, contact with CA beads; (3) rhC5a added, no contact with CA beads; and (4) rhC5a added, contact with CA beads. The concentration of plasma C5a before adding rhC5a was 6.9 ± 1.0 ng/mL, which is the baseline of C5a. After incubation, each aliquot of plasma was separated by centrifugation, and the concentrations of IL-1ra and HGF were measured. The amount of IL-1ra in the four groups was: (1) 215.9 ± 15.9 pg/mL; (2) 332.1 ± 89.0 pg/mL; (3) 1379.2 ± 188.4 pg/mL; and (4) 937.0 ± 156.3 pg/mL. The highest amount of IL-1ra was in group 3 (rhC5a added, no contact with CA beads) (Fig. 3A). The amount of HGF in the four groups was: (1) 773.2 ± 24.5 pg/mL; (2) 704.5 ± 93.3 pg/mL; (3) 840.9 ± 67.0 pg/mL; and (4) 1156.3 ± 124.8 pg/mL. The highest amount of HGF was in group 4 (rhC5a added, contact with CA beads) and the amount in group 3 increased slightly, but the level was not significant compared to the control group (Fig. 3B). These results show that C5a increases anti-inflammatory substances in GM adsorption to CA beads and has different effects on IL-1ra and HGF generation. We conclude that C5a can induce IL-1ra release without adsorption, while HGF release requires adsorption to CA beads.

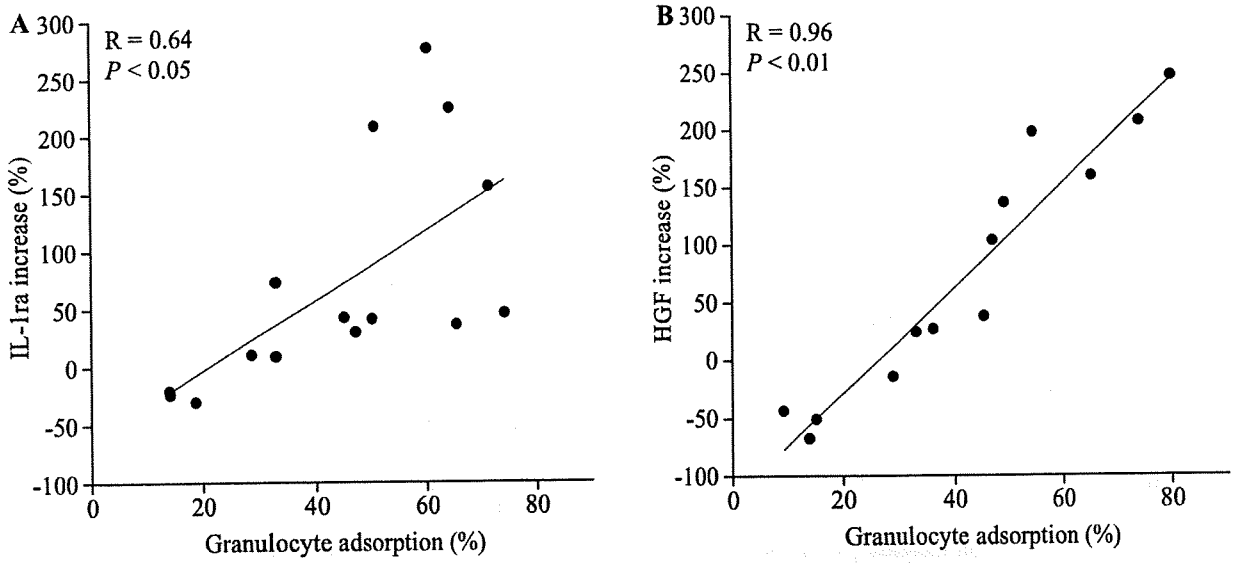

FIG. 2. Correlation of the increases in (A) interleukin-1 receptor antagonist (IL-1ra), and (B) hepatocyte growth factor (HGF) with granulocyte adsorption to cellulose acetate (CA) beads. Peripheral blood from healthy volunteers was mixed with serial dilutions of nafamostat mesilate and incubated with CA beads for 1 h. The fractions of granulocytes adsorbed to the CA beads were measured after incubation and then plasma was separated by centrifugation for measurement of IL-1ra and HGF. The ratio (%) of granulocyte adsorption and increase ratios (%) of IL-1ra and HGF were calculated as described in the Materials and Methods section. The *P* values are based on Spearman's rank correlation.

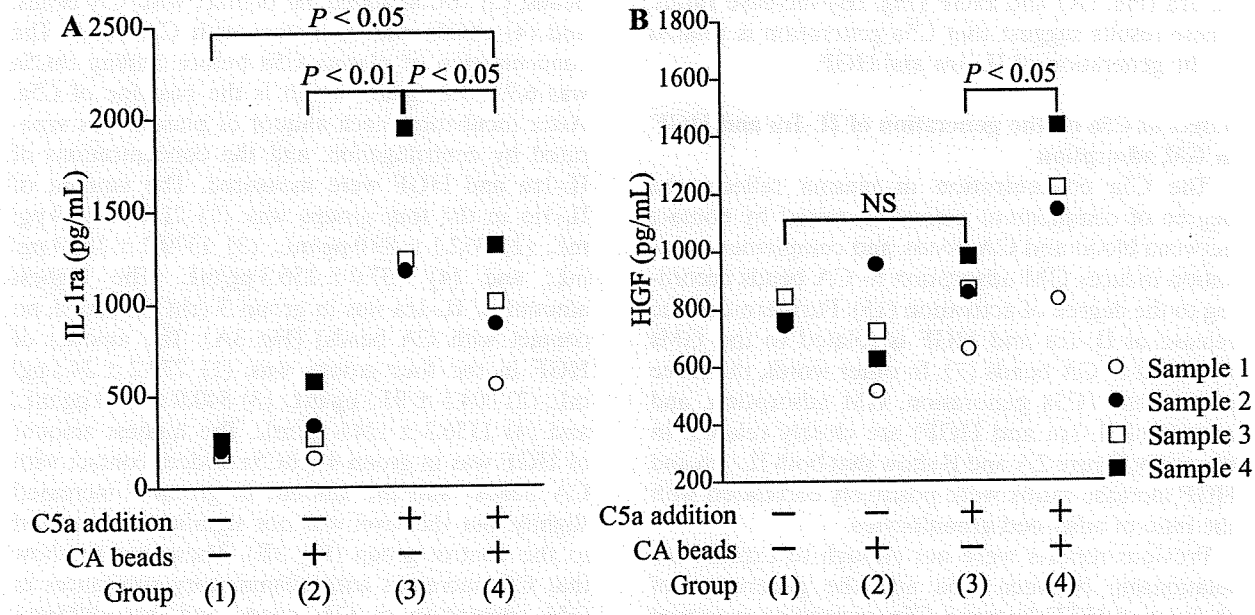

FIG. 3. Effect of recombinant human complement C5a (rhC5a) and cellulose acetate (CA) beads on (A) interleukin-1 receptor antagonist (IL-1ra), and (B) hepatocyte growth factor (HGF) generation. Peripheral blood containing 100 μmol/L nafamostat mesilate was divided into four groups: (1) no rhC5a added, no contact with CA beads (control group); (2) no rhC5a added, contact with CA beads; (3) 100 ng/mL rhC5a added, no contact with CA beads; and (4) 100 ng/mL rhC5a added, contact with CA beads. These were incubated for 1 h. After incubation, plasma was separated by centrifugation for measurement of IL-1ra and HGF. The *P* values are based on paired *t*-test.

DISCUSSION

CA beads are used for GMA therapy, and not only induce GM adsorption, but also generate C5a and the release of IL-1ra and HGF. These phenomena are interrelated; however, the precise role of C5a stimulation is still unclear. In this study we indicated that C5a can induce IL-1ra release without GM adsorption, and that C5a and GM adsorption to CA beads affect HGF release synergistically.

Activation and subsequent cleavage of C5 by C5 convertase produces the complement activation fragment C5a, an anaphylatoxin. Anaphylatoxins are involved in a variety of pro-inflammatory processes, and C5a has the strongest known biological effects (16). For example, because C5a induces the production of mediators that cause both vasodilatation and an increase in vascular permeability, it is partly responsible for the pathogenesis of sepsis, including hypovolemia due to both arterial and venous dilatation and leakage of plasma into the extravascular space (17–19). On the other hand, it is known that anaphylatoxins also have anti-inflammatory effects in some situations. C5a is essential during the early priming stages of hepatocyte regeneration in mice (21), and recombinant C5a induces the production of IL-1ra in peripheral mononuclear cells (22). In GM adsorption it has been reported that IL-1ra release is augmented by adding C5a (15). Additionally, an increase in HGF release by adding C5a was also revealed in this study. It has been reported that patients with UC, who responded to GM apheresis treatment, show a significant increase in IL-1ra in the Adacolumn outflow (9), and that HGF administration accelerates colonic mucosal repair in rats with dextran sulfate sodium-induced colitis (10). These reports suggest that IL-1ra and HGF might contribute to healing in UC patients. Thus, C5a produced during GMA is believed to provide clinical efficacy in patients with UC through an increase in anti-inflammatory substances.

In this study, both IL-1ra and HGF generation were augmented by adding rhC5a, but different experimental groups had the highest amount of each. The IL-1ra amount in group 3 (rhC5a added, no contact with CA beads) was the highest. Since IL-1ra increased by adding only rhC5a in the absence of CA beads, we believe that in GMA, the C5a produced by contact between blood and CA beads itself can induce IL-1ra generation from leukocytes without the stimulation of GM adsorption to CA beads. Strangely, the IL-1ra amount in group 4 (rhC5a added, contact with CA beads) was significantly lower than in group 3, although higher than in group 1 (no rhC5a added, no contact with CA beads). The reason why the presence of CA beads caused suppression of IL-1ra is unclear, though it might be that rhC5a or IL-1ra adsorbed to the CA beads. Further study of the effects of CA beads with respect to IL-1ra generation is necessary.

In contrast, the amount of HGF in group 4 was the highest. Since HGF did not significantly increase in the absence of CA beads, even in the presence of rhC5a, we believe that C5a, which itself induces little HGF generation from leukocytes, acts synergistically with CA beads to generate HGF. HGF is released by degranulation neutrophils (23), and adhesion-dependent degranulation of neutrophils requires Src family kinase (24). On the other hand, a C5a signal via the C5a receptor, known as a protein Gi-coupled seven membrane-spanning receptor, regulates Ras and mitogen-activated protein (MAP) kinase (25). The C5a signal cannot induce activation of the Src family. Thus, the stimulation caused by GM adsorption to CA beads may induce outside-in signals synergistically with C5a receptor signals and then induce Src family kinase phosphorylation.

CONCLUSION

The present study found that the generation of IL-1ra and HGF in GM adsorption was positively correlated with the degree of generation of anaphylatoxin C5a. C5a induced IL-1ra generation by itself and increased HGF generation synergistically with CA beads. Our results indicate that anaphylatoxin C5a plays important, anti-inflammatory roles in GMA therapy. This provides important insight into the various biological responses induced by GM adsorption and into understanding physiological anti-inflammatory responses.

Acknowledgments: We are grateful to Mr Okio Ohnuma, Mrs Fuyuko Kikuchi, Makiko Sato, Akiko Kamikawa, and Mr Kazunori Kanouchi for excellent technical assistance, and to the volunteers who contributed blood samples.

REFERENCES

1. Hanai H, Watanabe F, Saniabadi AR, Matsushitai I, Takeuchi K, Iida T. Therapeutic efficacy of granulocyte and monocyte adsorption apheresis in severe active ulcerative colitis. *Dig Dis Sci* 2002;47:2349–53.
2. Hanai H, Watanabe F, Takeuchi K et al. Leukocyte adsorptive apheresis for the treatment of active ulcerative colitis: a prospective, uncontrolled, pilot study. *Clin Gastroenterol Hepatol* 2003;1:28–35.
3. Ohara M, Saniabadi AR, Kokuma S et al. Granulocytapheresis in the treatment of patients with rheumatoid arthritis. *Artif Organs* 1997;21:989–94.

4. Takeda Y, Hiraishi K, Takeda H et al. Cellulose acetate beads induce release of interleukin-1 receptor antagonist, but not tumour necrosis factor-α or interleukin-1β in human peripheral blood. *Inflamm Res* 2003;52:287–90.
5. Saniabadi AR, Hanai H, Takeuchi K et al. Adacolumn, an adsorptive carrier based granulocyte and monocyte apheresis device for the treatment of inflammatory and refractory diseases associated with leukocytes. *Ther Apher Dial* 2003;7:48–59.
6. Hanai H, Iida T, Takeuchi K et al. Intensive granulocyte and monocyte adsorption versus intravenous prednisolone in patients with severe ulcerative colitis: an unblended randomized multi-centre controlled study. *Dig Liver Dis* 2008;40:433–40.
7. Takeda Y, Shiobara N, Saniabadi AR, Adachi M, Hiraishi K. Adhesion dependent release of hepatocyte growth factor and interleukin-1 receptor antagonist from human blood granulocytes and monocytes: evidence for the involvement of plasma IgG, complement C3 and β2 integrin. *Inflamm Res* 2004;53:277–83.
8. Arend WP, Malyak M, Guthridge CJ, Gabay C. Interleukin-1 receptor antagonist: role in biology. *Annu Rev Immunol* 1998;16:27–55.
9. Sakimura K, Omori T, Iwashita E et al. Clinical response is associated with elevated plasma interleukin-1 receptor antagonist during selective granulocyte and monocyte apheresis in patients with ulcerative colitis. *Dig Dis Sci* 2006;51:1525–31.
10. Tahara Y, Ido A, Yamamoto S et al. Hepatocyte growth factor facilitates colonic mucosal repair in experimental ulcerative colitis in rats. *J Pharmacol Exp Ther* 2003;307:146–51.
11. Hoenich NA, Woffindin C, Matthews JN, Goldfinch ME, Turnbull J. Clinical comparison of high-flux cellulose acetate and synthetic membranes. *Nephrol Dial Transplant* 1994;9:60–6.
12. Matata BM, Yin HQ, Courtney JM et al. In vitro blood compatibility evaluation of hollow fibre membrane using a controlled flow system: a comparative study. *Int J Artif Organs* 1996;19:582–9.
13. Ivanovich P, Chenoweth DE, Schmidt R et al. Cellulose acetate hemodialysis membranes are better tolerated than Cuprophan. A difference in complement and neutrophil activation. *Contrib Nephrol* 1984;37:78–82.
14. Hiraishi K, Takeda Y, Shiobara N et al. Studies on the mechanisms of leukocyte adhesion to cellulose acetate beads: an in vitro model to assess the efficacy of cellulose acetate carrier-based granulocyte and monocyte adsorptive apheresis. *Ther Apher Dial* 2003;7:334–40.
15. Nishise S, Takeda Y, Takeda H, Ishihama K, Fukui T, Kawata S. Complement activation is involved in biological responses to leukocyte adsorptive apheresis. *Dig Dis Sci* 2006;51:934–41.
16. Hartmann K, Henz BM, Kruger-Krasagakes S et al. C3a and C5a stimulate chemotaxis of human mast cells. *Blood* 1997;89:2863–70.
17. Stove S, Welte T, Wagner TOF et al. Circulating complement proteins in patients with sepsis or systemic inflammatory response syndrome. *Clin Diagn Lab Immunol* 1996;3:175–83.
18. Bjork J, Hugli TE, Smedegard G. Microvascular effects of anaphylatoxins C3a and C5a. *J Immunol* 1985;134:1115–19.
19. Vogt W. Anaphylatoxins: possible roles in disease. *Complement* 1986;3:177–88.
20. Belmont HM, Hopkins P, Edelson HS et al. Complement activation during systemic lupus erythematosus. C3a and C5a anaphylatoxins circulate during exacerbations of disease. *Arthritis Rheum* 1986;29:1085–9.
21. Strey CW, Markiewski M, Mastellos D et al. The proinflammatory mediators C3a and C5a are essential for liver regeneration. *J Exp Med* 2003;198:913–23.
22. Rousseau Y, Haeffner-Cavaillon N, Poignet JL, Meyrier A, Carreno MP. In vivo intracellular cytokine production by leukocytes during haemodialysis. *Cytokine* 2000;12:506–17.
23. Grenier A, Chollet-Martin S, Crestani B et al. Presence of a mobilizable intracellular pool of hepatocyte growth factor in human polymorphonuclear neutrophils. *Blood* 2002;99:2997–3004.
24. Mócsai A, Ligeti E, Lowell CA, Berton G. Adhesion-dependent degranulation of neutrophils requires the Src family kinases Fgr and Hck. *J Immunol* 1999;162:1120–6.
25. Buhl AM, Avdi N, Worthen GS, Johnson GL. Mapping of the C5a receptor signal transduction network in human neutrophils. *Proc Natl Acad Sci USA* 1994;91:9190–4.

JOURNAL OF VIROLOGY, Oct. 2009, p. 10427–10436 Vol. 83, No. 20
0022-538X/09/$08.00+0 doi:10.1128/JVI.01035-09

Cochaperone Activity of Human Butyrate-Induced Transcript 1 Facilitates Hepatitis C Virus Replication through an Hsp90-Dependent Pathway▽

Shuhei Taguwa,[1] Hiroto Kambara,[1] Hiroko Omori,[2] Hideki Tani,[1] Takayuki Abe,[1] Yoshio Mori,[1] Tetsuro Suzuki,[3] Tamotsu Yoshimori,[2] Kohji Moriishi,[1] and Yoshiharu Matsuura[1]*

Department of Molecular Virology[1] and Department of Cellular Regulation,[2] Research Institute for Microbial Diseases, Osaka University, Osaka, and Department of Virology II, National Institute of Infectious Diseases, Tokyo,[3] Japan

Received 21 May 2009/Accepted 27 July 2009

Hepatitis C virus (HCV) nonstructural protein 5A (NS5A) is a component of the replication complex consisting of several host and viral proteins. We have previously reported that human butyrate-induced transcript 1 (hB-ind1) recruits heat shock protein 90 (Hsp90) and FK506-binding protein 8 (FKBP8) to the replication complex through interaction with NS5A. To gain more insights into the biological functions of hB-ind1 in HCV replication, we assessed the potential cochaperone-like activity of hB-ind1, because it has significant homology with cochaperone p23, which regulates Hsp90 chaperone activity. The chimeric p23 in which the cochaperone domain was replaced with the p23-like domain of hB-ind1 exhibited cochaperone activity comparable to that of the authentic p23, inhibiting the glucocorticoid receptor signaling in an Hsp90-dependent manner. Conversely, the chimeric hB-ind1 in which the p23-like domain was replaced with the cochaperone domain of p23 resulted in the same level of recovery of HCV propagation as seen in the authentic hB-ind1 in cells with knockdown of the endogenous hB-ind1. Immunofluorescence analyses revealed that hB-ind1 was colocalized with NS5A, FKBP8, and double-stranded RNA in the HCV replicon cells. HCV replicon cells exhibited a more potent unfolded-protein response (UPR) than the parental and the cured cells upon treatment with an inhibitor for Hsp90. These results suggest that an Hsp90-dependent chaperone pathway incorporating hB-ind1 is involved in protein folding in the membranous web for the circumvention of the UPR and that it facilitates HCV replication.

Hepatitis C virus (HCV) is the major causative agent of non-A, non-B hepatitis in humans and infects approximately 170 million people worldwide (64). HCV belongs to the genus *Hepacivirus* of the family *Flaviviridae* and is classified into six major genotypes (39). The virus forms small, round, enveloped particles and possesses a genome consisting of a single positive-stranded RNA with a nucleotide length of 9.6 kb. The viral genome encodes a single precursor polyprotein consisting of approximately 3,000 amino acids, which in turn is posttranslationally processed into 10 viral proteins by host and viral proteases. The structural proteins are cleaved from the N-terminal one-fourth of the polyprotein by the host signal peptidase and signal peptide peptidase (36, 43, 44), resulting in the maturation of capsid protein, two envelope proteins, and viroporin p7. The nonstructural protein 2 (NS2) protease cleaves its own carboxyl terminus, and then NS3 cleaves the appropriate downstream positions to produce NS3, NS4A, NS4B, NS5A, and NS5B (24, 60), which form the replication complex, together with several host proteins (14, 35).

NS5A is a membrane-anchored zinc-binding phosphoprotein that appears to possess diverse functions, including the suppression of host defense and the regulation of virus replication (1, 15, 58), but its biological function remains unclear. Several groups, including ours, have suggested that the molecular chaperone, heat shock protein 90 (Hsp90), and several cochaperones participate in the replication complex of HCV through interaction with NS5A or other NS proteins (45, 56, 65). Hsp90 is the highly conserved and ubiquitously expressed protein that acts as a key regulator for the turnover and the activities of more than 200 signaling proteins, including steroid receptors and cell-signaling kinases (66). The chaperone activity of Hsp90 contributes to the refolding of an unfolded protein in an ATP-dependent manner, and the execution of Hsp90-dependent protein folding requires the formation of a multichaperone complex containing other chaperones (e.g., Hsp70, Hsp104, and Hsp40) and cochaperones (e.g., p23, Hop, and immunophilins) (4, 18, 48). Geldanamycin or its derivatives, which are represented as specific inhibitors of Hsp90, can destabilize and then degrade client proteins (41, 55).

The host chaperone mechanism is involved in the folding of viral polymerase to support viral replication (6, 27). Moreover, host chaperones have been reported to play roles in the assembly of viral particles and the sorting of virus proteins (9, 32, 38). We have previously reported that Hsp90 chaperone activities and chaperone-associated proteins are required for the efficient propagation of HCV (45, 56) and that human butyrate-induced transcript 1 (hB-ind1) is involved in the propagation of HCV through interactions with NS5A and Hsp90 via the coiled-coil domain and the FXXW motif, respectively (56). hB-ind1 was first reported to be a multiple-membrane-spanning protein consisting of 362 amino acids that possesses a significant homology with a cochaperones, p23, that regulates

* Corresponding author. Mailing address: Department of Molecular Virology, Research Institute for Microbial Diseases, Osaka University, 3-1, Yamadaoka, Suita-shi, Osaka 565-0871, Japan. Phone: 81-6-6879-8340. Fax: 81-6-6879-8269. E-mail: matsuura@biken.osaka-u.ac.jp.

▽ Published ahead of print on 5 August 2009.

Hsp90 function by its cochaperone activity (11). However, the roles of hB-ind1 in the life cycle of HCV have not been precisely clarified. In this study, we investigated the role of the Hsp90-related chaperone system, including hB-ind1, in the regulation of the RNA replication and particle production of HCV.

MATERIALS AND METHODS

Plasmids. The plasmids encoding hB-ind1, NS5A, Hsp90, and FK506-binding protein 8 (FKBP8) were prepared by methods described previously (45, 56). The DNA fragments encoding hB-ind1 mutants were prepared by PCR with the introduction of a silent mutation that is resistant to the short hairpin RNA in the hB-ind1 knockdown cells, as described previously (56). The human p23 gene and glucose-regulated protein 78 (GRP78) promoter region (−151 to +22) were amplified by PCR from the total cDNA and genomic DNA of Huh7 cells, respectively. The DNA fragments encoding mutants of hB-ind1 and p23 were prepared by the method of splicing by overlap extension (26) and introduced into pEF FLAGGs pGKpuro (28). The GRP78 promoter region was introduced between the KpnI and HindIII sites of pGL3-basic (Promega, Madison, WI) and designated pGRP78-luc. The reporter plasmid carrying a firefly luciferase gene under the control of the GR promoter (pGR-luc) was purchased from Panomics (Fremont, CA). The internal-control plasmid encoding a *Renilla* luciferase (pRL-TK) was purchased from Promega. The plasmid pFK-I_{389} neo/NS3-3′/NK5.1 (47) was kindly provided by R. Bartenschlager. The plasmids used in this study were confirmed by sequencing them with an ABI Prism 3130 genetic analyzer (Applied Biosystems, Tokyo, Japan).

Cells and virus infection. All cell lines were cultured at 37°C under a humidified atmosphere and 5% CO_2. The human embryonic kidney 293T and hepatocellular carcinoma Huh7 cell lines were maintained in Dulbecco's modified Eagle's medium (DMEM) (Sigma, St. Louis, MO) supplemented with 100 U/ml penicillin, 100 μg/ml streptomycin, and 10% fetal calf serum (FCS). The human hepatocellular carcinoma cell line Huh7.5.1 was kindly provided by F. Chisari (70) and was maintained in DMEM containing nonessential amino acids, 100 U/ml penicillin, 100 μg/ml streptomycin, and 10% FCS. The Huh9-13 cell line, which is a Huh7 cell line harboring a subgenomic HCV RNA replicon (35), was maintained in DMEM containing 10% FCS, nonessential amino acids, and 1 mg/ml G418 (Nakalai Tesque, Kyoto, Japan). The hB-ind1 knockdown cell line Huh-KD and control cell line Huh-ctrl were described previously (56). Huh-KD cells were transfected with each of the expression plasmids encoding wild-type or mutant hB-ind1 and cultured for 1 week in the presence of 10 μg/ml of puromycin. The remaining cells were used for the experiments described below. The viral RNA of JFH1 was introduced into Huh7.5.1 cells according to the method of Wakita et al. (62) for preparation of the infectious HCV particles in cell culture.

Antibodies. The rabbit anti-hB-ind1 antibody was prepared as described previously (56). Mouse monoclonal antibodies to HCV NS5A, influenza virus hemagglutinin (HA) and FLAG tags, and β-actin were purchased from Austral Biologicals (San Ramon, CA), Covance (Richmond, CA), and Sigma, respectively. Mouse anti-protein disulfide isomerase (PDI) immunoglobulin G2a (IgG2a) was from Affinity Bioreagents (Golden, CO). Mouse anti-double-stranded RNA (dsRNA) IgG2a (J1 and K2) antibodies were from Biocenter Ltd. (Szirak, Hungary). Alexa Fluor 488 (AF488)-conjugated anti-mouse IgG1, AF647-conjugated anti-rabbit IgG, and AF594-conjugated anti-mouse IgG2a and IgG2b antibodies were from Invitrogen (San Diego, CA).

Transfection, immunoblotting, and immunoprecipitation. Transfection and immunoprecipitation analyses were carried out as described previously (25, 45). Immunoprecipitates boiled in loading buffer were subjected to 12.5% sodium dodecyl sulfate-polyacrylamide gel electrophoresis. The proteins were transferred to polyvinylidene difluoride membranes (Millipore, Bedford, MA) and were reacted with the appropriate antibodies. The immune complexes were visualized with Super Signal West Femto substrate (Pierce, Rockford, IL) and detected by an LAS-3000 image analyzer system (Fujifilm, Tokyo, Japan). The protein bands of GRP78 and β-actin were quantified by Multi Gauge software (Fujifilm), and the values of GRP78 expression were normalized with those of β-actin.

Quantitative reverse transcriptase PCR. HCV RNA was estimated by the method described previously (56). Total RNA was prepared from cells by using an RNeasy minikit (Qiagen, Tokyo, Japan). First-strand cDNA was synthesized using an RNA LA PCR in vitro cloning kit (Takara Bio Inc., Shiga, Japan) and random primers. Each cDNA was estimated with Platinum SYBR green qPCR SuperMix UDG (Invitrogen) according to the manufacturer's protocol. Fluorescent signals were analyzed with an ABI Prism 7000 (Applied Biosystems). The internal ribosomal entry site regions of HCV and mRNAs of GAPDH (glyceraldehyde-3-phosphate dehydrogenase), GRP78, and growth arrest- and DNA damage-inducible gene 153 (GADD153) were amplified using the primer pairs 5′-GAGTGTCGTGCAGCCTCCA-3′ and 5′-CACTCGCAAGCACCCTATCA-3′, 5′-GAAGGTGAAGGTCGGAGTC-3′ and 5′-GAAGGTGAAGGTCGGAGTC-3′, 5′-CGCCAAGCGGCTCATC-3′ and 5′-AACCACCTTGAACGGCAAGA-3′, and 5′-AGCTGGAACCTGAGGAGAGA-3′ and 5′-TGGATCAGTCTGGAAAAGCA-3′, respectively. The values of the HCV genome or each mRNA were normalized with those of GAPDH mRNA. Each PCR product was detected as a single band of the correct size on agarose gel electrophoresis (data not shown).

In vitro transcription and RNA transfection. The plasmid pFK-I_{389} neo/NS3-3′/NK5.1 was linearized by treatment with ScaI and then transcribed in vitro using the MEGAscript T7 kit (Applied Biosystems) according to the manufacturer's protocol. The in vitro-transcribed RNA was electroporated into cells at 4 million cells/0.4 ml under conditions of 270 V and 960 μF using a Gene Pulser (Bio-Rad, Hercules, CA). The colony formation assay was carried out by a method described previously (45).

Indirect immunofluorescence assay. Cells cultured on glass slides were fixed with 4% paraformaldehyde in phosphate-buffered saline (PBS) at room temperature for 30 min. After being washed twice with PBS, the cells were permeabilized for 20 min at room temperature with PBS containing 0.25% saponin and blocked with PBS containing 0.2% gelatin (gelatin-PBS) for 60 min at room temperature. The cells were incubated with gelatin-PBS containing rabbit anti-hB-ind1 antibody, mouse anti-NS5A IgG1, mouse anti-PDI IgG2a, mouse anti-FKBP8 IgG2b, or mouse anti-dsRNA IgG2a (J1 and K2) at 37°C for 60 min; washed three times with PBS containing 1% Tween 20; and incubated with gelatin-PBS containing AF488-conjugated anti-mouse IgG1 or AF647-conjugated anti-rabbit or AF594-conjugated anti-mouse IgG2a or IgG2b antibodies at 37°C for 60 min. Finally, the cells were washed three times with PBS containing 1% Tween 20 and observed with a FluoView FV1000 laser scanning confocal microscope (Olympus, Tokyo, Japan).

Correlative FM-EM. Correlative fluorescence microscopy-electron microscopy (FM-EM) allows individual cells to be examined both in an overview with FM and in a detailed subcellular-structure view with EM (51). The endogenous hB-ind1 and NS5A were stained and observed in the HCV replicon cells by the correlative FM-EM method as described previously (45).

Luciferase assay. Each plasmid was transfected into Huh7, Huh9-13, and interferon (IFN)-cured cells seeded in a 12-well plate, and the cells were treated with 1 μM dexamethasone (Sigma) for 12 h or with 17-dimethylamino-ethylamino-17-demethoxygeldanamycin (DMAG) (Sigma) for 6 h at 36 h posttransfection and lysed in 200 μl of passive lysis buffer (Promega). Luciferase activity was measured in 20-μl aliquots of the cell lysates using a Dual-Luciferase Reporter Assay System (Promega). Firefly luciferase activity was standardized with that of *Renilla* luciferase cotransfected with the internal-control plasmid pRL-TK. The resulting values were expressed as the increase in relative light units (RLU).

Statistical analysis. Results were expressed as the mean ± standard deviation. The significance of differences in the means was determined by Student's *t* test.

RESULTS

The p23-like domain of hB-ind1 has cochaperone activity. Although we had previously reported that hB-ind1 regulates HCV RNA replication through interaction with NS5A and Hsp90, the molecular mechanisms underlying the regulation of HCV replication remained to be clarified. To gain more insights into the potential cochaperone activity of hB-ind1 in the Hsp90 chaperone system, we prepared expression plasmids encoding a wild-type p23 and three p23 mutants—one in which the FXXW motif was replaced with AXXA (p23AxxA), one in which the cochaperone domain of p23 was replaced with the p23-like domain of hB-ind1 (cp23), and one in which both substitutions were made (cp23AxxA) (Fig. 1A). HA-tagged Hsp90 was coexpressed with FLAG-tagged p23 or the FLAG-tagged p23 mutants in 293T cells (Fig. 1B). Hsp90 was coimmunoprecipitated with wild-type p23 and a cp23 mutant, but not with the p23AxxA or cp23AxxA mutants, indicating that the FXXW motif of hB-ind1, as is the case with that of p23

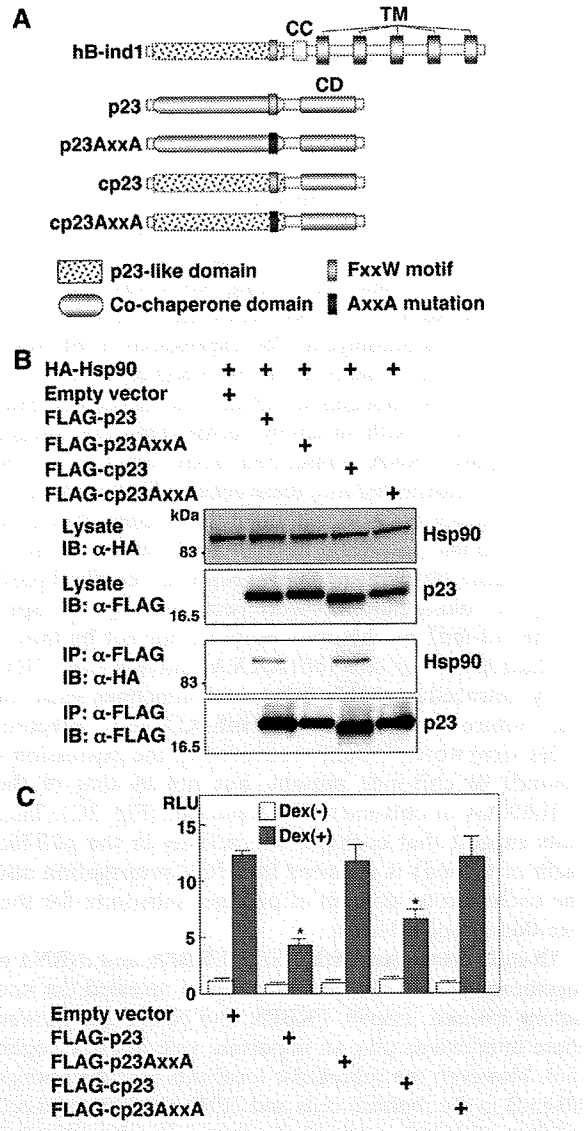

FIG. 1. Construction and characterization of p23 mutants. (A) Structures of hB-ind1, p23, and the three p23 mutants. hB-ind1 consists of a p23-like domain, an FXXW motif, a coiled-coil domain (CC), and a transmembrane domain (TM). p23 consists of a cochaperone domain, an FXXW motif, and a chaperone domain (CD). The three p23 mutants, p23AxxA, cp23, and cp23AxxA, were constructed by replacing the FXXW motif with AXXA, the cochaperone domain of p23 with the p23-like domain of hB-ind1, and both of the regions, respectively. (B) FLAG-tagged p23, p23AxxA, cp23, or cp23AxxA was coexpressed with HA-tagged Hsp90 in 293T cells and immunoprecipitated (IP) with anti-FLAG antibody. The immunoprecipitates were subjected to immunoblotting (IB). (C) The expression plasmid encoding FLAG-tagged p23, cp23, p23AxxA, or cp23AxxA was cotransfected with pGR-luc and pRL-TK plasmids into 293T cells and treated with 1 mM dexamethasone [Dex(+)] at 36 h posttransfection or untreated [Dex(−)], and the luciferase activities were determined at 12 h of incubation. The firefly luciferase activity was normalized with that of *Renilla* luciferase, and the GR-responsive promoter activity was indicated as the RLU. The error bars indicate standard deviations. The asterisks indicate significant differences ($P < 0.01$) versus the control value. The data shown are representative of three independent experiments.

(67), is also involved in binding to Hsp90. Hsp90 participates in the folding and stabilization of the ligand-binding domain of the glucocorticoid receptor (GR), together with p23 and other cofactors (49). p23 was shown to act not only in the activation (30), but also in the inhibition, of GR signaling (67). To examine whether hB-ind1 has the ability to work as a cochaperone in an Hsp90-dependent manner, each of the plasmids encoding p23 or the p23 mutants was cotransfected with a reporter plasmid carrying a firefly luciferase gene under the control of the GR promoter (pGR-luc), together with an internal-control plasmid (pRL-TK), and GR-mediated transcriptional activity was determined at 12 h after treatment with dexamethasone, a ligand of GR. Expression of the p23 or cp23 mutant, but not of the AXXA mutants, significantly inhibited GR-mediated transcription (Fig. 1C). These results indicate that the p23-like domain of hB-ind1 possesses cochaperone activity comparable to that of p23.

The p23-like domain of hB-ind1 is interchangeable with the p23 cochaperone domain during complex formation with NS5A, Hsp90, and FKBP8. Previous reports have suggested that HCV NS5A interacts with several host proteins, including FBL2 (63), vesicle-associated membrane protein-associated protein subtype A (VAP-A) (61), VAP-B (25), FKBP8 (45), and hB-ind1 (56), and that these interactions participate in the replication of HCV. We have shown that hB-ind1 interacts with NS5A and Hsp90 through the coiled-coil domain and the FXXW motif in the p23-like domain, respectively, and that coexpression of FKBP8 enhances the interaction of Hsp90 with hB-ind1 (56). To determine the effect of the mutation in the p23-like domain of hB-ind1 on interaction with Hsp90, NS5A, and FKBP8, we prepared an expression plasmid encoding wild-type hB-ind1 and three hB-ind1 mutants, one in which the p23-like domain was replaced with the cochaperone domain of p23 (chB-ind1), one in which the FXXW motif was replaced with AXXA (hB-ind1AxxA), and one in which both replacements were made (chB-ind1AxxA) (Fig. 2A). The FLAG-tagged wild-type or mutant hB-ind1 was coexpressed with HA-tagged Hsp90 (Fig. 2B, left) or HA-tagged NS5A (Fig. 2B, right) in 293T cells and immunoprecipitated with anti-FLAG antibody. Hsp90 was coprecipitated with wild-type hB-ind1 and the chB-ind1 mutant, but not with the hB-ind1AXXA and chB-ind1AXXA mutants (Fig. 2B, left), confirming that the FXXW motif is crucial for the interaction with Hsp90. In contrast, NS5A was coprecipitated with each of the hB-ind1 proteins, suggesting that mutation in the p23-like domain of hB-ind1 has no effect on the binding of hB-ind1 to NS5A through the coiled-coil domain (Fig. 2B, right). To determine the effect of FKBP8 expression on the interaction between hB-ind1 and Hsp90, FLAG-tagged wild-type hB-ind1 or the chB-ind1 mutant was coexpressed with HA-tagged FKBP8 and/or Hsp90 in 293T cells and immunoprecipitated with anti-FLAG antibody. The amounts of Hsp90 coprecipitated with hB-ind1 or chB-ind1 were increased by coexpression of FKBP8 (Fig. 2C). To further examine the interaction of hB-ind1 with Hsp90 and NS5A at an endogenous expression level in Huh9-13 cells harboring an HCV subgenomic RNA replicon, lysates of the replicon cells were subjected to immunoprecipitation analysis. Endogenous Hsp90 and NS5A were specifically coimmunoprecipitated with endogenous hB-ind1 (Fig. 2D). These results suggest that the p23-like domain of hB-ind1 is inter-

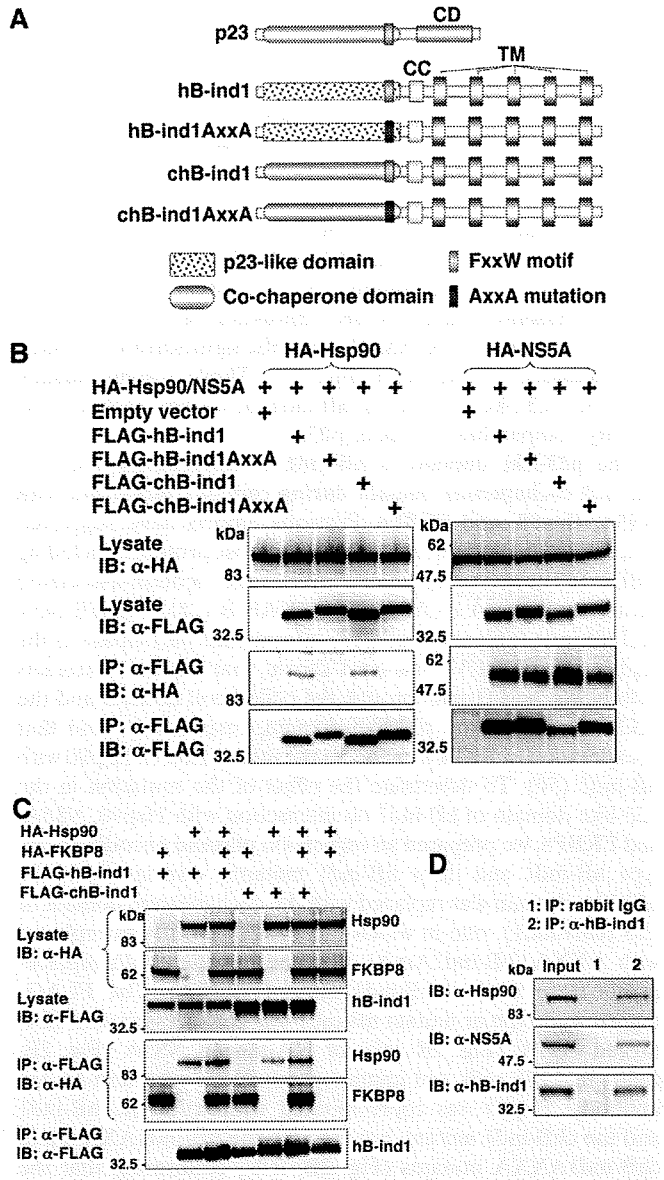

FIG. 2. Construction and characterization of hB-ind1 mutants. (A) Structures of p23, hB-ind1, and the three hB-ind1 mutants. The three hB-ind1 mutants, hB-ind1AxxA, chB-ind1, and chB-ind1AxxA, were constructed by replacing the FXXW motif with AXXA, the p23-like domain of hB-ind1 with the cochaperone domain of p23, and both of the regions, respectively. (B) FLAG-tagged hB-ind1, hB-ind1 AxxA, chB-ind1, or chB-ind1AxxA was coexpressed with either HA-tagged Hsp90 (left) or NS5A (right) in 293T cells and immunoprecipitated (IP) with anti-FLAG antibody. The immunoprecipitates were subjected to immunoblotting (IB). (C) HA-tagged Hsp90 and HA-FKBP8 were expressed with FLAG-tagged hB-ind1 and chB-ind1 in various combinations in 293T cells and immunoprecipitated with anti-FLAG antibody, and the immunoprecipitates were detected by immunoblotting. (D) Endogenous hB-ind1 in Huh9-13 cells harboring subgenomic HCV replicon RNA was immunoprecipitated with anti-hB-ind1 rabbit IgG (lane 2). The cell lysate was mixed with normal rabbit IgG as a negative control (lane 1). The immunoprecipitates were analyzed by immunoblotting with an antibody to Hsp90, NS5A, or hB-ind1. The data shown are representative of three independent experiments.

changeable with the cochaperone domain of p23 during complex formation with NS5A, Hsp90, and FKBP8.

Cochaperone activity in the p23-like domain of hB-ind1 is required for propagation of HCV. The p23-like domain of hB-ind1 has been suggested to be required for HCV propagation (56). However, the involvement of the cochaperone activity of hB-ind1 in HCV propagation has not been examined. To assess the effect of cochaperone activity in the p23-like domain of hB-ind1 on the RNA replication and particle production of HCV, each of the expression plasmids encoding the FLAG-tagged wild-type or mutant hB-ind1 carrying the silent mutations resistant to small interfering RNA was transfected into hB-ind1 knockdown (Huh-KD) cells and cultured for a week in the presence of puromycin. The expressions of FLAG-tagged hB-ind1 and the mutants in the Huh-KD cells were comparable to that of the endogenous hB-ind1 in the control (Huh-ctrl) cells transfected with an empty vector (Fig. 3A). Subgenomic HCV replicon RNA transcribed from pFK-I_{389} neo/NS3-3′/NK5.1 was transfected into these cells and cultured for 4 weeks in the presence of G418. Although the number of colonies was reduced in the Huh-KD cells compared with the Huh-ctrl cells after transfection with an empty vector, as described previously (56), the colony numbers were recovered by the expression of the hB-ind1 or chB-ind1 mutant, but not by that of the hB-ind1AXXA or chB-ind1AXXA mutants (Fig. 3B). Similarly, intracellular HCV RNA and infectious viral titers in the culture supernatants of Huh-KD cells infected with JFH1 virus were partially recovered by the expression of the hB-ind1 or chB-ind1 mutant, but not by that of the hB-ind1AXXA or chB-ind1AXXA mutant (Fig. 3C). These results suggest that cochaperone activity in the p23-like domain of hB-ind1 is required for HCV propagation and that the cochaperone domain of p23 can substitute for the p23-like domain of hB-ind1.

hB-ind1 colocalizes with NS5A, FKBP8, and dsRNA on the membranous web. Our previous report revealed the interplay among hB-ind1, Hsp90, FKBP8, and NS5A and showed that these interactions play an important role in HCV replication (56). However, the subcellular localization of the endogenous hB-ind1 in the replicon cells and JFH1 virus-infected cells has not been precisely assessed. To determine the subcellular localization of hB-ind1 in the context of HCV replication, the expression of hB-ind1 and NS5A in the replicon cells and JFH1 virus-infected cells was examined by immunofluorescence analyses (Fig. 4A). Endogenous hB-ind1 was colocalized with the endoplasmic reticulum (ER)-marker PDI and NS5A as dot-like structures in the Huh9-13 replicon cells (Fig. 4A, top) and in cells infected with JFH1 virus (Fig. 4A, bottom), and these dot-like structures disappeared in concert with the loss of NS5A expression by treatment with IFN-α in the replicon cells and was not observed in the mock-infected Huh7.5.1 cells. Furthermore, FKBP8 (Fig. 4B, top) and dsRNA (Fig. 4B, bottom) were colocalized with hB-ind1 and NS5A in the dot-like structures in Huh9-13 replicon cells. These results indicate that HCV replicating RNA is localized with hB-ind1, FKBP8, and NS5A in the dot-like compartments. HCV RNA replication or expression of viral proteins leads to formation of the convoluted membranous structures designated the membranous web (14, 23). The large structures of the replication complexes in the replicon cells indicate membranous webs with

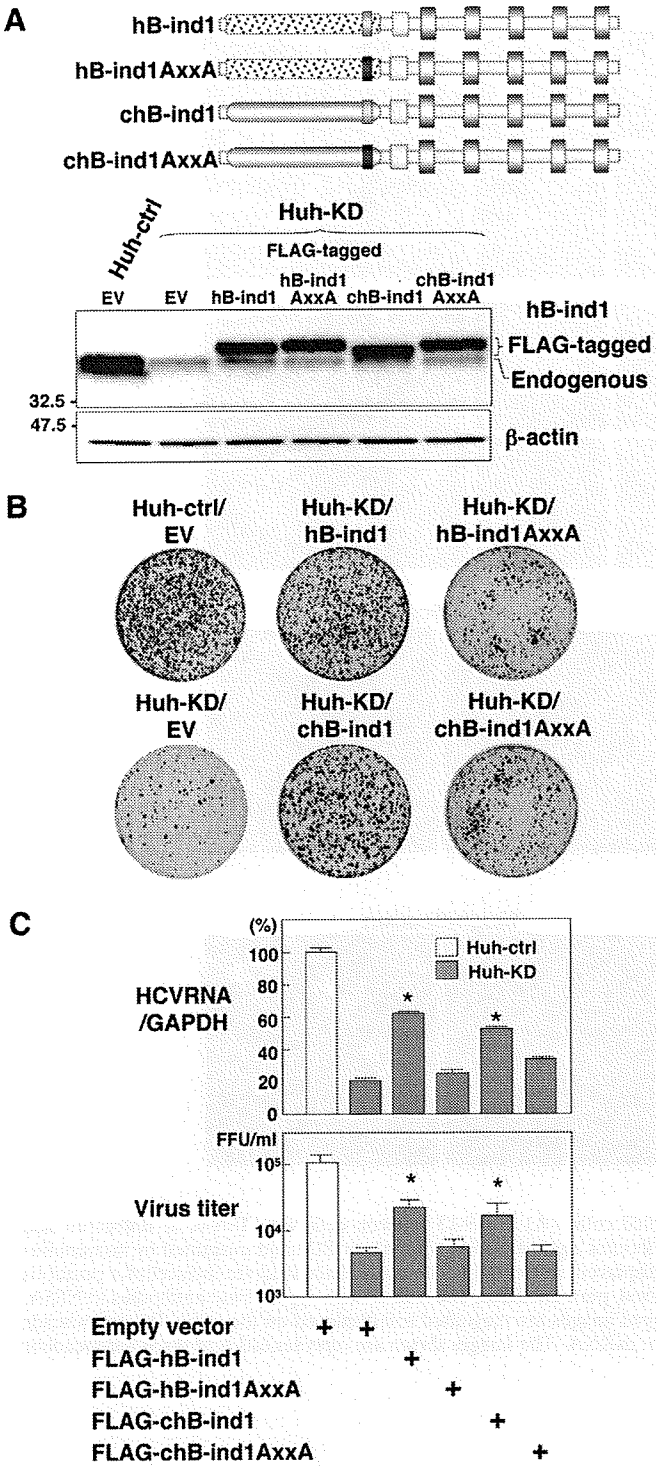

FIG. 3. Effects of the cochaperone activity of hB-ind1 on the propagation of HCV. (A) Huh-KD cells were transfected with either an empty vector or an expression plasmid encoding FLAG-tagged hB-ind1, hB-ind1AxxA, chB-ind1, or chB-ind1AxxA, which are resistant to small interfering RNA due to the introduction of silent mutations, and cultured for a week in the presence of 10 μg/ml of puromycin. The surviving cells were used in the subsequent experiments. The endogenous and exogenous expression of hB-ind1 and the mutants was detected by immunoblotting. The control cell line (Huh-ctrl) or the Huh-KD cell line transfected with an empty vector (EV) was used as a control. (B) Huh-KD cells were transfected with the plasmids and then selected with puromycin. The resulting cells were further transfected with a replicon RNA transcribed from pFK-I_{389} neo/NS3-3′/NK5.1, cultured for 4 weeks in the presence of 1 mg/ml of G418, and stained with crystal violet after fixation with 4% paraformaldehyde. The Huh-KD cell line transfected with an empty vector (EV) was used as a positive control. (C) The cells prepared as described above were infected with JFH1 virus and harvested at 3 days postinfection. The amount of intracellular HCV RNA was estimated by quantitative reverse transcriptase PCR and normalized with that of GAPDH mRNA. The values of HCV RNA are presented as percentages versus those of Huh-ctrl cells transfected with an empty vector. The culture supernatants were subjected to a focus-forming assay. Virus titers are presented as focus-forming units (FFU) per ml. The error bars indicate standard deviations. The asterisks indicate significant differences ($P < 0.01$) versus the value of the control. The data shown are representative of three independent experiments.

restricted motility (68). To further analyze the subcellular compartments, including hB-ind1 and NS5A, the same field of the Huh9-13 replicon cells was observed under FM and EM by using the correlative FM-EM technique (Fig. 5A, upper two rows). The large structures that included hB-ind1 and NS5A in the replicon cells were observed under FM and EM (white-boxed areas) and further magnified (black-boxed areas). Convoluted membranous structures that consisted of small vesicles and that were similar to the membranous web were observed. Another field of view yielded similar results (Fig. 5A, lower two rows). The membranous web resembling the convoluted structures was not observed in the Huh9-13 cells depleted of viral RNA by IFN treatment (Fig. 5B). Together, these results suggest that hB-ind1 interacts with NS5A on the membranous web in cells replicating HCV RNA.

Hsp90 is involved in the circumvention of the UPR during HCV replication. Hsp90 regulates the folding and stability of proteins in all eukaryotes (59), and inhibition of the chaperone pathway suppresses correct protein folding, which leads to induction of proteasome-mediated degradation of the unfolded proteins and the unfolded protein response (UPR). Our previous (46) and present studies (Fig. 4 and 5) showed that several cochaperone components are recruited in the membranous web, suggesting that the Hsp90 chaperone system participates in the replication complex to circumvent the induction of the UPR and to maintain the folding of the host and viral proteins in a replication-competent state. To determine the induction of the UPR by HCV replication, Huh9-13 replicon cells were transfected with a reporter plasmid carrying a firefly luciferase gene under the control of the GRP78 promoter, which is activated by the induction of the UPR, together with an internal-control plasmid. Although the GRP78 promoter activity was slightly enhanced in the Huh9-13 cells compared to that in the parental cells, a fourfold increase of GRP78 promoter activity in the replicon cells was observed after treatment with an Hsp90 inhibitor, DMAG, in contrast to the twofold increase in similarly treated parental Huh7 cells, and the activation of the GRP78 promoter was canceled by treatment with IFN-α despite DMAG treatment (Fig. 6A), suggesting that the Hsp90 chaperone system participates in the circumvention of the UPR induced by the replication of HCV RNA. In addition, activation of GRP78 at transcriptional and translational levels after treatment with DMAG was higher in the

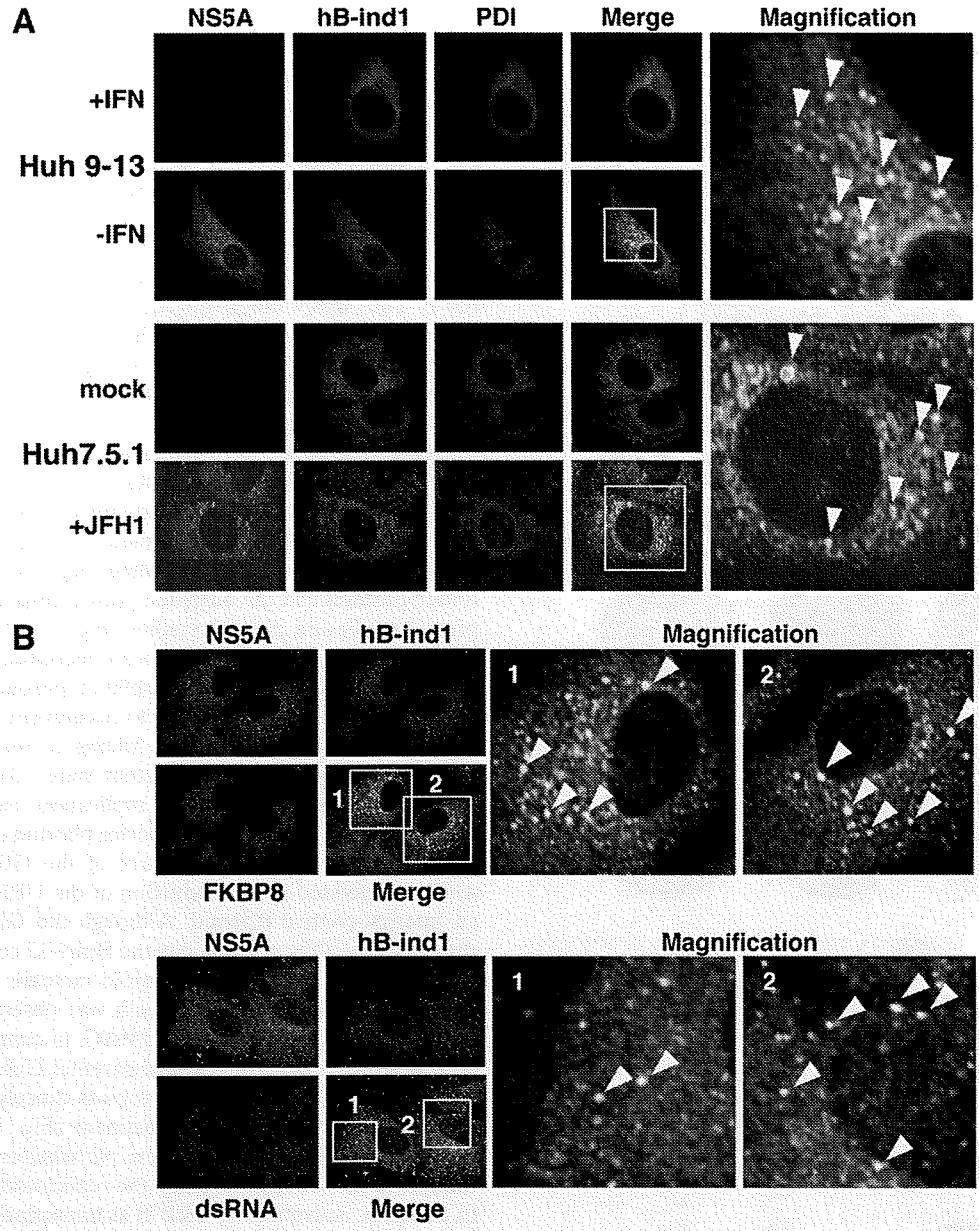

FIG. 4. Intracellular localization of hB-ind1 in replicon cells and infected cells. (A) Huh9-13 replicon cells with IFN-α or untreated and Huh7.5.1 cells infected with JFH1 virus or naïve cells were stained with antibodies against NS5A, hB-ind1, or PDI and examined by immunofluorescence assay. The boxed areas in the merged images are magnified and displayed on the right. The arrowheads indicate intracellular positions colocalized with NS5A, hB-ind1, and PDI. (B) Huh9-13 replicon cells were fixed, permeabilized, and stained with appropriate antibodies to NS5A, hB-ind1, and FKBP8 (top) or dsRNA (bottom). The boxed areas in the merged images are magnified and displayed on the right. The arrowheads indicate intracellular positions colocalized with NS5A, hB-ind, and FKBP8 or dsRNA. The images shown are representative of three independent experiments.

HCV replicon cells than in the parental cells or in cured cells, which were depleted of HCV RNA by treatment with IFN-α (Fig. 6B). Furthermore, DMAG treatment enhanced the transcription of the UPR marker protein GADD153 at a higher level in the replicon cells than in the parental Huh7 or the cured cells (Fig. 6C). These results suggest that the Hsp90-dependent chaperone system plays a crucial role in the folding of the host and viral proteins involved in HCV replication and in the regulation of UPR induction.

DISCUSSION

Studies of the relationship between Hsp90 and steroid receptors, such as GR, have revealed the activities of cochaperones (52, 67). Cochaperones, such as p23, appear to interact with and dissociate from Hsp90 and the client protein complex in a defined order. These cochaperones participate in the chaperone complex in a late step and promote the dissociation of the client proteins from Hsp90 to facilitate formation of the

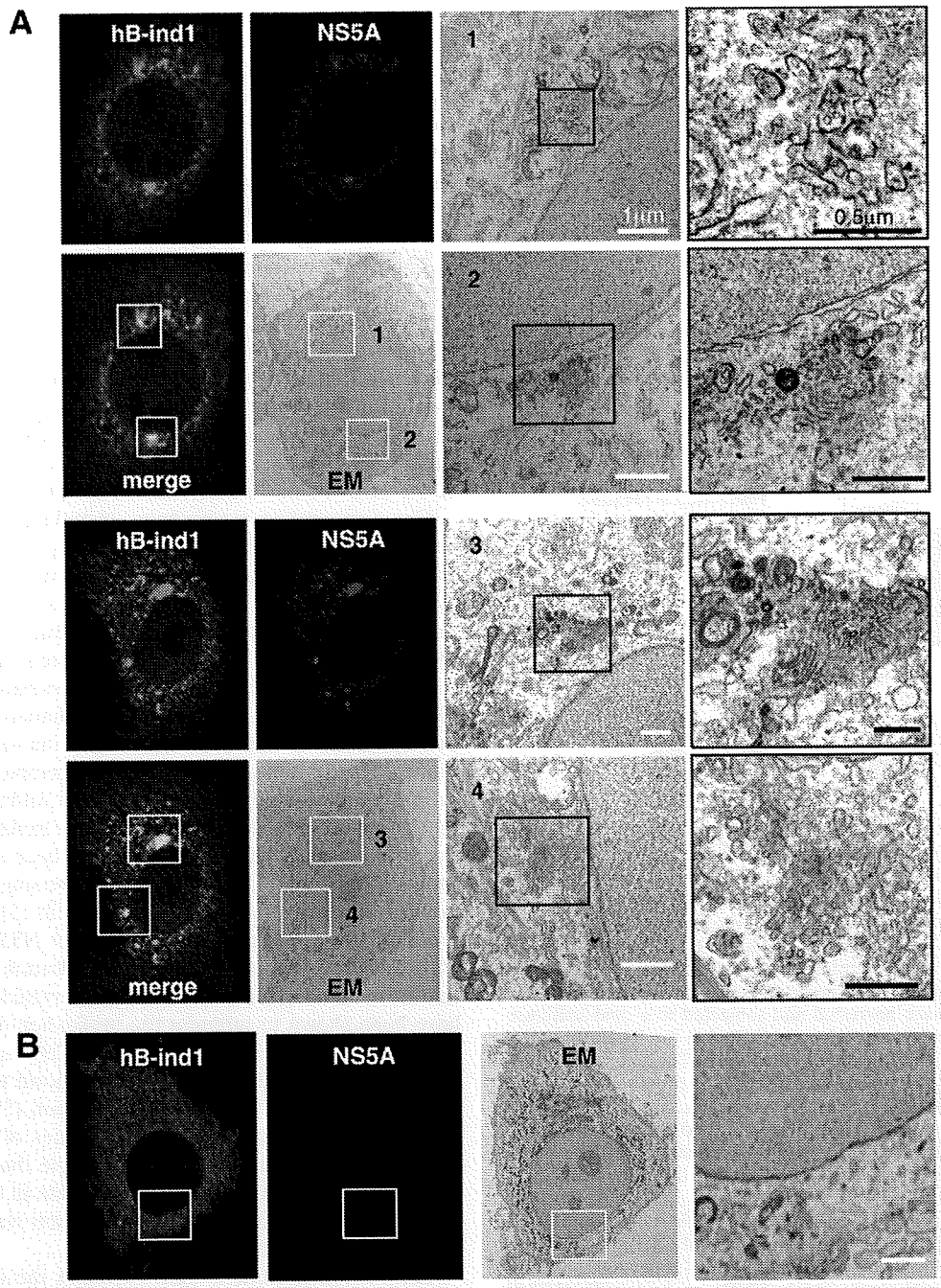

FIG. 5. hB-ind1 interacts with NS5A in the membranous web. Huh9-13 replicon cells were stained with specific antibodies to hB-ind1 and NS5A. Identical fields of Huh9-13 (A) or the cured cells (B) were observed under EM by using the correlative FM-EM technique. The white-boxed areas indicate the colocalized areas of hB-ind1 with NS5A. Magnified views of the white-boxed areas are displayed in the third column from the left. The right column contains further-magnified images of each of the black-boxed areas. Another field of view is presented in the lower two rows.

chaperone complex in the next chaperone cycle (16–18). In this study, we have shown that hB-ind1 participates in HCV replication and that the p23-like domain of hB-ind1 possesses cochaperone activity comparable to that of the cochaperone domain of p23, suggesting that hB-ind1 is involved in the recycling of the chaperone complex in the membranous web to maintain the function of the replication complex of HCV.

Previous studies have indicated that HCV proteins rearrange the ER membrane into the small convoluted membranous vesicles that are collectively known as the membranous web, and these vesicles have been suggested to be the intracellular compartments in which HCV replication takes place (14, 23, 68). In the living replicon cells, two forms of replication complexes, small and large vesicles, are detected, both of which include the viral replication complexes (68). Large vesicles, corresponding to membranous webs, exhibit restricted motil-

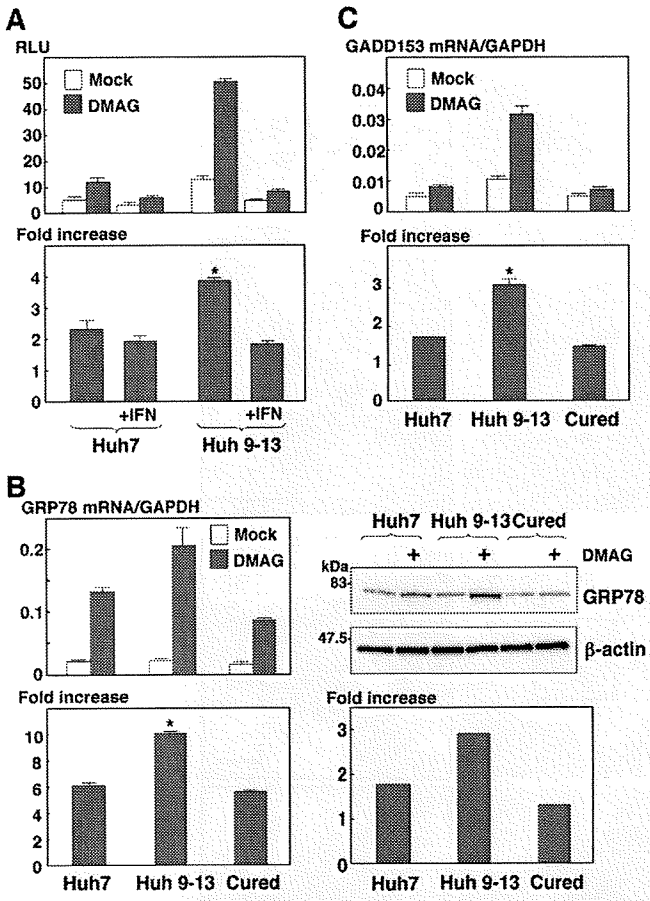

FIG. 6. Effect of Hsp90 inhibitor on the induction of the UPR in HCV replicon cells. (A) Huh7 and Huh9-13 replicon cells were transfected with a reporter plasmid, pGRP78-luc, and an internal-control plasmid, pRL-TK. The transfected cells were treated with IFN-α (+IFN) from 6 to 36 h posttransfection or left untreated and then further incubated for 6 h in the presence or absence of 1 μM DMAG. The resulting cells were harvested and subjected to a dual-luciferase assay. The firefly luciferase activity is indicated as the RLU (top) after standardization with that of *Renilla* luciferase. The enhancement of promoter activity by treatment with DMAG is presented as the increase (bottom). (B) Huh7 cells, Huh9-13 cells, and Huh9-13 cells cured by IFN-α treatment (Cured) were cultured for 6 h in the presence or absence of 1 μM DMAG, and the amount of GRP78 mRNA was measured by real-time PCR. The value of the mRNA was normalized with the amount of GAPDH mRNA (upper left), and the transcriptional enhancement by treatment with DMAG is presented as the increase (lower left). The expression levels of GRP78 and β-actin in the cells were determined by immunoblotting (upper right) and are presented as the increase (lower right). (C) The amounts of GADD153 mRNA in Huh7 cells, Huh9-13 cells, and the cured cells cultured for 6 h in the presence or absence of 1 μM DMAG were measured by real-time PCR. The values of the mRNA were normalized with the amount of GAPDH mRNA (top), and the transcriptional enhancement by treatment with DMAG is presented as the increase (bottom). The error bars indicate standard deviations. The asterisks indicate significant differences ($P < 0.01$) versus the control value. The data shown are representative of three independent experiments.

ity, while small vesicles show fast movement (68), and FM and EM have revealed that NS5A is colocalized with hB-ind1, as well as FKBP8 (45), in the membranous webs. hB-ind1 was first identified as a regulator of Rac1 that activates JNK and NF-κB (11). Rac1 is a member of the Rho GTPase family and plays crucial roles in cytoskeletal dynamics, membrane ruffling, and gene transcription through the effectors of the Rho GTPase family members. IQGAP1 and PAK1 are Rac1 effectors that bind to Rac proteins and are also involved in the replication of HCV (5, 7, 19, 31, 50). The tetratricopeptide repeat domain of immunophilin family members, such as FKBP8, has been shown to interact with Hsp90 (12, 45) and the GR-Hsp90 complex that leads to association with dynein for retrograde transport, along with microtubules (12). Hsp90 has been shown to play an important role in the interaction of transcriptase with genomic RNA of hepatitis B virus (27) and the nuclear transportation of the polymerase of influenza virus (40). Flock house virus also recruits Hsp90 in the polymerase synthesis in the early step of infection (9). Hsp90 may be involved in the regulation of the movement and arrangement of the HCV replication complexes through interaction with Rac1, hB-ind1, and FKBP8. Further investigation is needed to clarify the role of the Hsp90 chaperone system in the life cycle of HCV.

The surrounding membranes, including the membranous web, may protect the viral replication complex and RNA genome against digestion by the host proteases and nucleases (69). The replication complex is composed of viral nonstructural proteins and host proteins, including chaperone and cochaperone proteins. HCV NS5A has been shown to interact with various host proteins, including cochaperones, such as FKBP8 and hB-ind1, and to recruit a chaperone, Hsp90, into the replication complex through interaction with these cochaperones. Recruitment of the chaperone complex into the replication complex is crucial for the correct folding of newly synthesized viral proteins to maintain the efficient replication of the viral genome. HCV replication has been shown to be improved by the adaptive mutations suppressing the phosphorylation status of NS5A in the replicon cells (3). Although suppression of the hyperphosphorylation of NS5A by treatment with kinase inhibitors improves the replication of the replicons that have no adaptive mutations (42), several kinase inhibitors have been shown to suppress the replication of the HCV replicon carrying the adaptive mutations (29), and phosphorylation of NS5A by casein kinase II was shown to improve virus production but not HCV RNA replication (57). Hsp90 is capable of directly modulating the activities of several kinases (37, 53, 54), and thus, it might be feasible that cochaperones, including hB-ind1 and FKBP8, participate in the propagation of HCV by regulating the phosphorylation status of NS5A in cooperation with Hsp90.

The host chaperone system regulates the quality of client proteins, and impairment of the chaperone activity induces accumulation of misfolded proteins and affects the natural cellular function and viability (20, 21, 33). In this study, DMAG treatment induced a higher level of UPR in HCV replicon cells than in parental and cured cells, indicating that the Hsp90 chaperone system participates in the maintenance of correct folding of the viral and host proteins in the replication complex in the membranous web and in the circumvention of the UPR induced by HCV replication. Treatment with geldanamycin or its derivatives has been shown to inhibit GRP94, which is the Hsp90 paralog located in the ER (10), and to disrupt the ER chaperone pathway, leading to the induction of ER-associated protein degradation, transcriptional attenuation, and eventually induction of apoptosis (34). ER chaperones, such as

GRP94, may also participate in the correct folding of the viral and host proteins in the replication complex for efficient replication of the HCV genome.

Geldanamycin and its derivatives have been reported to remarkably inhibit poliovirus replication in vivo without any emergence of drug-resistant escape mutants (22), suggesting that an inhibitor of the chaperone system may be a promising candidate for the treatment of viral infectious diseases with low risk of the emergence of drug-resistant viruses. In addition, Hsp90 inhibitors exhibit anticancer activities through the suppression of various cell signals essential for cancer growth and the enhancement of radiation sensitivity (2, 8, 13). In conclusion, our data indicate that hB-ind1 is included within the HCV replication complex and regulates HCV RNA replication through its own cochaperone activity. Hsp90 and cochaperones, including hB-ind1 and FKBP8, which are required for efficient HCV replication, should be ideal targets for the treatment of chronic hepatitis C with a low frequency of emergence of drug-resistant breakthrough viruses.

ACKNOWLEDGMENTS

We thank H. Murase for her secretarial work. We also thank R. Bartenschlager, T. Wakita, and F. V. Chisari for providing the plasmids and cell lines.

This work was supported in part by grants-in-aid from the Ministry of Health, Labor, and Welfare; the Ministry of Education, Culture, Sports, Science, and Technology; the Global Center of Excellence Program; the Foundation for Biomedical Research and Innovation; and the Naito Foundation.

REFERENCES

1. **Abe, T., Y. Kaname, I. Hamamoto, Y. Tsuda, X. Wen, S. Taguwa, K. Moriishi, O. Takeuchi, T. Kawai, T. Kanto, N. Hayashi, S. Akira, and Y. Matsuura.** 2007. Hepatitis C virus nonstructural protein 5A modulates the toll-like receptor-MyD88-dependent signaling pathway in macrophage cell lines. J. Virol. **81**:8953–8966.
2. **Bisht, K. S., C. M. Bradbury, D. Mattson, A. Kaushal, A. Sowers, S. Markovina, K. L. Ortiz, L. K. Sieck, J. S. Isaacs, M. W. Brechbiel, J. B. Mitchell, L. M. Neckers, and D. Gius.** 2003. Geldanamycin and 17-allylamino-17-demethoxygeldanamycin potentiate the in vitro and in vivo radiation response of cervical tumor cells via the heat shock protein 90-mediated intracellular signaling and cytotoxicity. Cancer Res. **63**:8984–8995.
3. **Blight, K. J., A. A. Kolykhalov, and C. M. Rice.** 2000. Efficient initiation of HCV RNA replication in cell culture. Science **290**:1972–1974.
4. **Bohen, S. P., A. Kralli, and K. R. Yamamoto.** 1995. Hold 'em and fold 'em: chaperones and signal transduction. Science **268**:1303–1304.
5. **Bost, A. G., D. Venable, L. Liu, and B. A. Heinz.** 2003. Cytoskeletal requirements for hepatitis C virus (HCV) RNA synthesis in the HCV replicon cell culture system. J. Virol. **77**:4401–4408.
6. **Brown, G., H. W. Rixon, J. Steel, T. P. McDonald, A. R. Pitt, S. Graham, and R. J. Sugrue.** 2005. Evidence for an association between heat shock protein 70 and the respiratory syncytial virus polymerase complex within lipid-raft membranes during virus infection. Virology **338**:69–80.
7. **Bryan, B. A., D. Li, X. Wu, and M. Liu.** 2005. The Rho family of small GTPases: crucial regulators of skeletal myogenesis. Cell Mol. Life Sci. **62**: 1547–1555.
8. **Calderwood, S. K., M. A. Khaleque, D. B. Sawyer, and D. R. Ciocca.** 2006. Heat shock proteins in cancer: chaperones of tumorigenesis. Trends Biochem. Sci. **31**:164–172.
9. **Castorena, K. M., S. A. Weeks, K. A. Stapleford, A. M. Cadwallader, and D. J. Miller.** 2007. A functional heat shock protein 90 chaperone is essential for efficient flock house virus RNA polymerase synthesis in *Drosophila* cells. J. Virol. **81**:8412–8420.
10. **Chavany, C., E. Mimnaugh, P. Miller, R. Bitton, P. Nguyen, J. Trepel, L. Whitesell, R. Schnur, J. Moyer, and L. Neckers.** 1996. p185erbB2 binds to GRP94 in vivo. Dissociation of the p185erbB2/GRP94 heterocomplex by benzoquinone ansamycins precedes depletion of p185erbB2. J. Biol. Chem. **271**:4974–4977.
11. **Courilleau, D., E. Chastre, M. Sabbah, G. Redeuilh, A. Atfi, and J. Mester.** 2000. B-ind1, a novel mediator of Rac1 signaling cloned from sodium butyrate-treated fibroblasts. J. Biol. Chem. **275**:17344–17348.
12. **Davies, T. H., Y. M. Ning, and E. R. Sanchez.** 2002. A new first step in activation of steroid receptors: hormone-induced switching of FKBP51 and FKBP52 immunophilins. J. Biol. Chem. **277**:4597–4600.
13. **Didelot, C., D. Lanneau, M. Brunet, A. L. Joly, A. De Thonel, G. Chiosis, and C. Garrido.** 2007. Anti-cancer therapeutic approaches based on intracellular and extracellular heat shock proteins. Curr. Med. Chem. **14**:2839–2847.
14. **Egger, D., B. Wolk, R. Gosert, L. Bianchi, H. E. Blum, D. Moradpour, and K. Bienz.** 2002. Expression of hepatitis C virus proteins induces distinct membrane alterations including a candidate viral replication complex. J. Virol. **76**:5974–5984.
15. **Evans, M. J., C. M. Rice, and S. P. Goff.** 2004. Genetic interactions between hepatitis C virus replicons. J. Virol. **78**:12085–12089.
16. **Freeman, B. C., S. J. Felts, D. O. Toft, and K. R. Yamamoto.** 2000. The p23 molecular chaperones act at a late step in intracellular receptor action to differentially affect ligand efficacies. Genes Dev. **14**:422–434.
17. **Freeman, B. C., and K. R. Yamamoto.** 2002. Disassembly of transcriptional regulatory complexes by molecular chaperones. Science **296**:2232–2235.
18. **Frydman, J., and J. Hohfeld.** 1997. Chaperones get in touch: the Hip-Hop connection. Trends Biochem. Sci. **22**:87–92.
19. **Fukata, M., M. Nakagawa, and K. Kaibuchi.** 2003. Roles of Rho-family GTPases in cell polarisation and directional migration. Curr. Opin. Cell Biol. **15**:590–597.
20. **Garrido, C., M. Brunet, C. Didelot, Y. Zermati, E. Schmitt, and G. Kroemer.** 2006. Heat shock proteins 27 and 70: anti-apoptotic proteins with tumorigenic properties. Cell Cycle **5**:2592–2601.
21. **Garrido, C., S. Gurbuxani, L. Ravagnan, and G. Kroemer.** 2001. Heat shock proteins: endogenous modulators of apoptotic cell death. Biochem. Biophys. Res. Commun. **286**:433–442.
22. **Geller, R., M. Vignuzzi, R. Andino, and J. Frydman.** 2007. Evolutionary constraints on chaperone-mediated folding provide an antiviral approach refractory to development of drug resistance. Genes Dev. **21**:195–205.
23. **Gosert, R., D. Egger, V. Lohmann, R. Bartenschlager, H. E. Blum, K. Bienz, and D. Moradpour.** 2003. Identification of the hepatitis C virus RNA replication complex in Huh-7 cells harboring subgenomic replicons. J. Virol. **77**:5487–5492.
24. **Grakoui, A., D. W. McCourt, C. Wychowski, S. M. Feinstone, and C. M. Rice.** 1993. Characterization of the hepatitis C virus-encoded serine proteinase: determination of proteinase-dependent polyprotein cleavage sites. J. Virol. **67**:2832–2843.
25. **Hamamoto, I., Y. Nishimura, T. Okamoto, H. Aizaki, M. Liu, Y. Mori, T. Abe, T. Suzuki, M. M. Lai, T. Miyamura, K. Moriishi, and Y. Matsuura.** 2005. Human VAP-B is involved in hepatitis C virus replication through interaction with NS5A and NS5B. J. Virol. **79**:13473–13482.
26. **Ho, S. N., H. D. Hunt, R. M. Horton, J. K. Pullen, and L. R. Pease.** 1989. Site-directed mutagenesis by overlap extension using the polymerase chain reaction. Gene **77**:51–59.
27. **Hu, J., D. Flores, D. Toft, X. Wang, and D. Nguyen.** 2004. Requirement of heat shock protein 90 for human hepatitis B virus reverse transcriptase function. J. Virol. **78**:13122–13131.
28. **Huang, D. C., S. Cory, and A. Strasser.** 1997. Bcl-2, Bcl-XL and adenovirus protein E1B19kD are functionally equivalent in their ability to inhibit cell death. Oncogene **14**:405–414.
29. **Huang, Y., K. Staschke, R. De Francesco, and S. L. Tan.** 2007. Phosphorylation of hepatitis C virus NS5A nonstructural protein: a new paradigm for phosphorylation-dependent viral RNA replication? Virology **364**:1–9.
30. **Hutchison, K. A., L. F. Stancato, J. K. Owens-Grillo, J. L. Johnson, P. Krishna, D. O. Toft, and W. B. Pratt.** 1995. The 23-kDa acidic protein in reticulocyte lysate is the weakly bound component of the hsp foldosome that is required for assembly of the glucocorticoid receptor into a functional heterocomplex with hsp90. J. Biol. Chem. **270**:18841–18847.
31. **Ishida, H., K. Li, M. Yi, and S. M. Lemon.** 2007. p21-activated kinase 1 is activated through the mammalian target of rapamycin/p70 S6 kinase pathway and regulates the replication of hepatitis C virus in human hepatoma cells. J. Biol. Chem. **282**:11836–11848.
32. **Kampmueller, K. M., and D. J. Miller.** 2005. The cellular chaperone heat shock protein 90 facilitates Flock House virus RNA replication in *Drosophila* cells. J. Virol. **79**:6827–6837.
33. **Kim, H. P., D. Morse, and A. M. Choi.** 2006. Heat-shock proteins: new keys to the development of cytoprotective therapies. Exp. Opin. Ther. Targets **10**:759–769.
34. **Lai, E., T. Teodoro, and A. Volchuk.** 2007. Endoplasmic reticulum stress: signaling the unfolded protein response. Physiology **22**:193–201.
35. **Lohmann, V., F. Korner, J. Koch, U. Herian, L. Theilmann, and R. Bartenschlager.** 1999. Replication of subgenomic hepatitis C virus RNAs in a hepatoma cell line. Science **285**:110–113.
36. **McLauchlan, J., M. K. Lemberg, G. Hope, and B. Martoglio.** 2002. Intramembrane proteolysis promotes trafficking of hepatitis C virus core protein to lipid droplets. EMBO J. **21**:3980–3988.
37. **Miyata, Y., and I. Yahara.** 1992. The 90-kDa heat shock protein, HSP90, binds and protects casein kinase II from self-aggregation and enhances its kinase activity. J. Biol. Chem. **267**:7042–7047.
38. **Momose, F., T. Naito, K. Yano, S. Sugimoto, Y. Morikawa, and K. Nagata.**

2002. Identification of Hsp90 as a stimulatory host factor involved in influenza virus RNA synthesis. J. Biol. Chem. **277**:45306–45314.
39. **Moradpour, D., F. Penin, and C. M. Rice.** 2007. Replication of hepatitis C virus. Nat. Rev. Microbiol. **5**:453–463.
40. **Naito, T., F. Momose, A. Kawaguchi, and K. Nagata.** 2007. Involvement of Hsp90 in assembly and nuclear import of influenza virus RNA polymerase subunits. J. Virol. **81**:1339–1349.
41. **Neckers, L.** 2002. Hsp90 inhibitors as novel cancer chemotherapeutic agents. Trends Mol. Med. **8**:S55–S61.
42. **Neddermann, P., M. Quintavalle, C. Di Pietro, A. Clementi, M. Cerretani, S. Altamura, L. Bartholomew, and R. De Francesco.** 2004. Reduction of hepatitis C virus NS5A hyperphosphorylation by selective inhibition of cellular kinases activates viral RNA replication in cell culture. J. Virol. **78**:13306–13314.
43. **Okamoto, K., Y. Mori, Y. Komoda, T. Okamoto, M. Okochi, M. Takeda, T. Suzuki, K. Moriishi, and Y. Matsuura.** 2008. Intramembrane processing by signal peptide peptidase regulates the membrane localization of hepatitis C virus core protein and viral propagation. J. Virol. **82**:8349–8361.
44. **Okamoto, K., K. Moriishi, T. Miyamura, and Y. Matsuura.** 2004. Intramembrane proteolysis and endoplasmic reticulum retention of hepatitis C virus core protein. J. Virol. **78**:6370–6380.
45. **Okamoto, T., Y. Nishimura, T. Ichimura, K. Suzuki, T. Miyamura, T. Suzuki, K. Moriishi, and Y. Matsuura.** 2006. Hepatitis C virus RNA replication is regulated by FKBP8 and Hsp90. EMBO J. **25**:5015–5025.
46. **Okamoto, T., H. Omori, Y. Kaname, T. Abe, Y. Nishimura, T. Suzuki, T. Miyamura, T. Yoshimori, K. Moriishi, and Y. Matsuura.** 2008. A single-amino-acid mutation in hepatitis C virus NS5A disrupting FKBP8 interaction impairs viral replication. J. Virol. **82**:3480–3489.
47. **Pietschmann, T., V. Lohmann, A. Kaul, N. Krieger, G. Rinck, G. Rutter, D. Strand, and R. Bartenschlager.** 2002. Persistent and transient replication of full-length hepatitis C virus genomes in cell culture. J. Virol. **76**:4008–4021.
48. **Prapapanich, V., S. Chen, E. J. Toran, R. A. Rimerman, and D. F. Smith.** 1996. Mutational analysis of the hsp70-interacting protein Hip. Mol. Cell. Biol. **16**:6200–6207.
49. **Pratt, W. B., and D. O. Toft.** 1997. Steroid receptor interactions with heat shock protein and immunophilin chaperones. Endocr. Rev. **18**:306–360.
50. **Ridley, A. J., H. F. Paterson, C. L. Johnston, D. Diekmann, and A. Hall.** 1992. The small GTP-binding protein rac regulates growth factor-induced membrane ruffling. Cell **70**:401–410.
51. **Rieder, C. L., and S. S. Bowser.** 1985. Correlative immunofluorescence and electron microscopy on the same section of epon-embedded material. J. Histochem. Cytochem. **33**:165–171.
52. **Sanchez, E. R., D. O. Toft, M. J. Schlesinger, and W. B. Pratt.** 1985. Evidence that the 90-kDa phosphoprotein associated with the untransformed L-cell glucocorticoid receptor is a murine heat shock protein. J. Biol. Chem. **260**:12398–12401.
53. **Sato, S., N. Fujita, and T. Tsuruo.** 2000. Modulation of Akt kinase activity by binding to Hsp90. Proc. Natl. Acad. Sci. USA **97**:10832–10837.
54. **Stancato, L. F., A. M. Silverstein, J. K. Owens-Grillo, Y. H. Chow, R. Jove, and W. B. Pratt.** 1997. The hsp90-binding antibiotic geldanamycin decreases Raf levels and epidermal growth factor signaling without disrupting formation of signaling complexes or reducing the specific enzymatic activity of Raf kinase. J. Biol. Chem. **272**:4013–4020.
55. **Stravopodis, D. J., L. H. Margaritis, and G. E. Voutsinas.** 2007. Drug-mediated targeted disruption of multiple protein activities through functional inhibition of the Hsp90 chaperone complex. Curr. Med. Chem. **14**: 3122–3138.
56. **Taguwa, S., T. Okamoto, T. Abe, Y. Mori, T. Suzuki, K. Moriishi, and Y. Matsuura.** 2008. Human butyrate-induced transcript 1 interacts with hepatitis C virus NS5A and regulates viral replication. J. Virol. **82**:2631–2641.
57. **Tellinghuisen, T. L., K. L. Foss, and J. Treadaway.** 2008. Regulation of hepatitis C virion production via phosphorylation of the NS5A protein. PLoS Pathog. **4**:e1000032.
58. **Tellinghuisen, T. L., J. Marcotrigiano, and C. M. Rice.** 2005. Structure of the zinc-binding domain of an essential component of the hepatitis C virus replicase. Nature **435**:374–379.
59. **Terasawa, K., M. Minami, and Y. Minami.** 2005. Constantly updated knowledge of Hsp90. J. Biochem. **137**:443–447.
60. **Tomei, L., C. Failla, E. Santolini, R. De Francesco, and N. La Monica.** 1993. NS3 is a serine protease required for processing of hepatitis C virus polyprotein. J. Virol. **67**:4017–4026.
61. **Tu, H., L. Gao, S. T. Shi, D. R. Taylor, T. Yang, A. K. Mircheff, Y. Wen, A. E. Gorbalenya, S. B. Hwang, and M. M. Lai.** 1999. Hepatitis C virus RNA polymerase and NS5A complex with a SNARE-like protein. Virology **263**: 30–41.
62. **Wakita, T., T. Pietschmann, T. Kato, T. Date, M. Miyamoto, Z. Zhao, K. Murthy, A. Habermann, H. G. Krausslich, M. Mizokami, R. Bartenschlager, and T. J. Liang.** 2005. Production of infectious hepatitis C virus in tissue culture from a cloned viral genome. Nat. Med. **11**:791–796.
63. **Wang, C., M. Gale, Jr., B. C. Keller, H. Huang, M. S. Brown, J. L. Goldstein, and J. Ye.** 2005. Identification of FBL2 as a geranylgeranylated cellular protein required for hepatitis C virus RNA replication. Mol. Cell **18**:425–434.
64. **Wasley, A., and M. J. Alter.** 2000. Epidemiology of hepatitis C: geographic differences and temporal trends. Semin. Liver Dis. **20**:1–16.
65. **Watashi, K., N. Ishii, M. Hijikata, D. Inoue, T. Murata, Y. Miyanari, and K. Shimotohno.** 2005. Cyclophilin B is a functional regulator of hepatitis C virus RNA polymerase. Mol. Cell **19**:111–122.
66. **Whitesell, L., and S. L. Lindquist.** 2005. HSP90 and the chaperoning of cancer. Nat. Rev. Cancer. **5**:761–772.
67. **Wochnik, G. M., J. C. Young, U. Schmidt, F. Holsboer, F. U. Hartl, and T. Rein.** 2004. Inhibition of GR-mediated transcription by p23 requires interaction with Hsp90. FEBS Lett. **560**:35–38.
68. **Wolk, B., B. Buchele, D. Moradpour, and C. M. Rice.** 2008. A dynamic view of hepatitis C virus replication complexes. J. Virol. **82**:10519–10531.
69. **Yang, G., D. C. Pevear, M. S. Collett, S. Chunduru, D. C. Young, C. Benetatos, and R. Jordan.** 2004. Newly synthesized hepatitis C virus replicon RNA is protected from nuclease activity by a protease-sensitive factor(s). J. Virol. **78**:10202–10205.
70. **Zhong, J., P. Gastaminza, G. Cheng, S. Kapadia, T. Kato, D. R. Burton, S. F. Wieland, S. L. Uprichard, T. Wakita, and F. V. Chisari.** 2005. Robust hepatitis C virus infection in vitro. Proc. Natl. Acad. Sci. USA **102**:9294–9299.

JOURNAL OF VIROLOGY, Mar. 2009, p. 2389–2392 Vol. 83, No. 5
0022-538X/09/$08.00+0 doi:10.1128/JVI.01690-08

Proteasomal Turnover of Hepatitis C Virus Core Protein Is Regulated by Two Distinct Mechanisms: a Ubiquitin-Dependent Mechanism and a Ubiquitin-Independent but PA28γ-Dependent Mechanism▽

Ryosuke Suzuki,[1] Kohji Moriishi,[2] Kouichirou Fukuda,[1] Masayuki Shirakura,[1] Koji Ishii,[1] Ikuo Shoji,[3] Takaji Wakita,[1] Tatsuo Miyamura,[1] Yoshiharu Matsuura,[2] and Tetsuro Suzuki[1]*

Department of Virology II, National Institute of Infectious Diseases, Tokyo 162-8640,[1] Department of Molecular Virology, Research Institute for Microbial Diseases, Osaka University, Osaka 565-0871,[2] and Division of Microbiology, Kobe University Graduate School of Medicine, Hyogo 650-0017,[3] Japan

Received 8 August 2008/Accepted 5 December 2008

We have previously reported on the ubiquitylation and degradation of hepatitis C virus core protein. Here we demonstrate that proteasomal degradation of the core protein is mediated by two distinct mechanisms. One leads to polyubiquitylation, in which lysine residues in the N-terminal region are preferential ubiquitylation sites. The other is independent of the presence of ubiquitin. Gain- and loss-of-function analyses using lysineless mutants substantiate the hypothesis that the proteasome activator PA28γ, a binding partner of the core, is involved in the ubiquitin-independent degradation of the core protein. Our results suggest that turnover of this multifunctional viral protein can be tightly controlled via dual ubiquitin-dependent and -independent proteasomal pathways.

Hepatitis C virus (HCV) core protein, whose amino acid sequence is highly conserved among different HCV strains, not only is involved in the formation of the HCV virion but also has a number of regulatory functions, including modulation of signaling pathways, cellular and viral gene expression, cell transformation, apoptosis, and lipid metabolism (reviewed in references 9 and 15). We have previously reported that the E6AP E3 ubiquitin (Ub) ligase binds to the core protein and plays an important role in polyubiquitylation and proteasomal degradation of the core protein (22). Another study from our group identified the proteasome activator PA28γ/REG-γ as an HCV core-binding partner, demonstrating degradation of the core protein via a PA28γ-dependent pathway (16, 17). In this work, we further investigated the molecular mechanisms underlying proteasomal degradation of the core protein and found that in addition to regulation by the Ub-mediated pathway, the turnover of the core protein is also regulated by PA28γ in a Ub-independent manner.

Although ubiquitylation of substrates generally requires at least one Lys residue to serve as a Ub acceptor site (5), there is no consensus as to the specificity of the Lys targeted by Ub (4, 8). To determine the sites of Ub conjugation in the core protein, we used site-directed mutagenesis to replace individual Lys residues or clusters of Lys residues with Arg residues in the N-terminal 152 amino acids (aa) of the core (C152), within which is contained all seven Lys residues (Fig. 1A). Plasmids expressing a variety of mutated core proteins were generated by PCR and inserted into the pCAGGS (18). Each core-expressing construct was transfected into human embryonic kidney 293T cells along with the pMT107 (25) encoding a Ub moiety tagged with six His residues (His_6). Transfected cells were treated with the proteasome inhibitor MG132 for 14 h to maximize the level of Ub-conjugated core intermediates by blocking the proteasome pathway and were harvested 48 h posttransfection. His_6-tagged proteins were purified from the extracts by Ni^{2+}-chelation chromatography. Eluted protein and whole lysates of transfected cells before purification were analyzed by Western blotting using anticore antibodies (Fig. 1B). Mutations replacing one or two Lys residues with Arg in the core protein did not affect the efficiency of ubiquitylation: detection of multiple Ub-conjugated core intermediates was observed in the mutant core proteins comparable to the results seen with the wild-type core protein as previously reported (23). In contrast, a substitution of four N-terminal Lys residues (C152K6-23R) caused a significant reduction in ubiquitylation (Fig. 1B, lane 9). Multiple Ub-conjugated core intermediates were not detected in the Lys-less mutant (C152KR), in which all seven Lys residues were replaced with Arg (Fig. 1B, lane 11). These results suggest that there is not a particular Lys residue in the core protein to act as the Ub acceptor but that more than one Lys located in its N-terminal region can serve as the preferential ubiquitylation site. In rare cases, Ub is known to be conjugated to the N terminus of proteins; however, these results indicate that this does not occur within the core protein.

To investigate how polyubiquitylation correlates with proteasome degradation of the core protein, we performed kinetic analysis of the wild-type and mutated core proteins by use of the Ub protein reference (UPR) technique, which can compensate for data scatter of sample-to-sample variations such as levels of expression (10, 24). Fusion proteins expressed from UPR-based constructs (Fig. 2A) were cotranslationally cleaved by deubiquitylating enzymes, thereby generating equimolar quantities of the core proteins and the reference protein, dihydrofolate reductase-hemagglutinin (DHFR-HA) tag-modified Ub, in which the Lys at aa 48 was replaced by Arg to prevent its polyubiquitylation (Ub^{R48}). After 24 h of transfec-

* Corresponding author. Mailing address: Department of Virology II, National Institute of Infectious Diseases, 1-23-1 Toyama, Shinjuku-ku, Tokyo 162-8640, Japan. Phone: 81-3-5285-1111. Fax: 81-3-5285-1161. E-mail: tesuzuki@nih.go.jp.
▽ Published ahead of print on 17 December 2008.